Characterisation of neonatal *Staphylococcus capitis* NRCS-A isolates compared with non NRCS-A *Staphylococcus capitis* from neonates and adults.

Heather Felgate[1,2], Dheeraj Sethi[1,3], Kirstin Faust[4], Cemsid Kiy[4], Christoph Härtel[5], Jan Rupp[6], Rebecca Clifford[2], Rachel Dean[1,3], Catherine Tremlett[3], John Wain[1,2], Gemma Langridge[1,2], Paul Clarke[2,3], Andrew Page[1], Mark A Webber[1,2*].

[1] Quadram Institute Bioscience, Norwich Research Park, NR4 7UQ, Norwich, UK

[2] Norwich Medical School, University of East Anglia (UEA), Norwich, UK

[3] Norfolk and Norwich University Hospital (NNUH), NR4 7UY, Norwich, UK

[4] Department of Pediatrics, University of Lübeck, Lübeck, Germany

[5] Department of Pediatrics, University of Würzburg, Würzburg, Germany

[6] Department of Infectious Diseases and Microbiology, University of Lübeck, Lübeck, Germany

[*]mark.webber@quadram.ac.uk

01603255233

Keywords: microbiota, skin, infection control, CRISPR, Antimicrobial Resistance, neonates, Late Onset Infection

Abstract

Staphylococcus capitis is a frequent cause of Late-Onset Sepsis (LOS) in neonates admitted to Neonatal Intensive Care Units (NICU). The NRCS-A clone of *S. capitis* has been isolated from NICUs globally although the reasons for the global success of this clone are not understood.

We analysed a collection of *S. capitis* colonising babies admitted to two NICUs, one in the UK and one in Germany as well as corresponding pathological clinical isolates. Genome analysis identified 3 groups; non-NRCS-A isolates, NRCS-A isolates, and a group of 'proto NRCS-A' - isolates closely related to NRCS-A but not associated with neonatal infection. All bloodstream isolates belonged to the NRCS-A group and were indistinguishable from strains carried on the skin or in the gut. NRCS-A isolates showed increased tolerance to chlorhexidine and antibiotics relative to the other *S. capitis* as well as enhanced ability to grow at higher pH values. Analysis of 138 pangenomes of the clades identified characteristic *nsr* and *tarJ* genes in the NRCS-A and proto groups with a CRISPR-cas system only seen in NRCS-A isolates which also showed enrichment of genes for metal acquisition and transport.

We found evidence for transmission of *S. capitis* NRCS-A within NICU, with related isolates shared between babies and multiple acquisitions by some babies. Our data show NRCS-A strains commonly colonise uninfected babies in NICU representing a potential reservoir for potential infection. This work provides more evidence that adaptation to survive in the gut and on skin facilitates spread of NRCS-A, and that metal acquisition and tolerance may be important to the biology of NRCS-A. Understanding how NRCS-A survives in NICUs can help develop infection control procedures against this clone.

Introduction

Non-*aureus* Staphylococci are common commensal bacteria, however many have also been implicated in nosocomial infections and are also found to cause Late Onset Sepsis (LOS). LOS is defined as sepsis occurring ≥ 72 hrs after birth which can be caused by various bacterial species, the most common being the Non-*aureus* Staphylococci (NAS) (Bentlin et al., 2010, Makhoul et al., 2005, Dong and Speer, 2014, Harvey et al., 2022). LOS increases the length of hospital stay, invasive procedures, and provokes more and longer antibiotic treatments all of which can have negative impacts on the long-term outcomes of new-born babies (Bentlin et al., 2010, Makhoul et al., 2005, Dong and Speer, 2014, Rasigade et al., 2012).

Staphylococcus capitis is a common commensal of humans and is regularly cultured from skin or nasal swabs (Becker et al., 2020), but a particular clone of *S. capitis* NRCS-A has been found to associated with LOS. Originally identified in France (the archetypal strain is known as CR01) it has subsequently been found in neonatal intensive care units (NICUs) in 17 countries (Lemriss et al., 2014, Lepainteur et al., 2013, Wirth et al., 2020, Butin et al., 2017, Harvey et al., 2022). Infection with NRCS-A has been associated with a higher morbidity and mortality than other NAS (Butin et al., 2019, Ben Said et al., 2016). The transmission routes of NRCS-A are not well understood but it has been documented to colonise incubators and equipment and has reduced susceptibility to antiseptics which has been proposed to aid its environmental survival. Unlike other NAS, infection with NRCS-A is not associated with maternal-fetal transmission, and babies born by Caesarean-section have been shown to be colonised more often than those delivered vaginally (Butin et al., 2019).

NRCS-A isolates typically have a multidrug resistance profile including methicillin, aminoglycosides and fosfomycin, hetero-resistance to vancomycin (a common treatment for LOS) and decreased susceptibility to chlorhexidine (Wirth et al., 2020, Lepainteur et al., 2013, Rasigade et al., 2012, Harvey et al., 2022). Many NRCS-A isolates have been found to contain a S*CCmec* mobile genetic element (*SCCmec-SCCcad-SCCars-SCCcop*) responsible for the methicillin resistance (Carter et al., 2018, Du et al., 2021, Becker et al., 2014) and decreased susceptibility to vancomycin has been associated with SNPs in *sarA* and *glnQ* (Wirth et al., 2020). Analysis of genomes of a panel of NRCS-A isolates from various sites and sources suggested the clone emerged in the 1960s before expanding in the 1980s with vancomycin use proposed as a major driver in the selection and evolution of NRCS-A (Wirth et al., 2020).

S. capitis infection has only been studied sporadically outside of the neonatal setting but *S. capitis* has been identified in bone and joint infections and, whilst rarely associated with adult disease, NRCS-A has been identified in endocarditis, osteomyelitis and prosthetic joint infections (PJI) in adults (Tevell et al., 2020).

71 Here we report results from a longitudinal survey of NAS from skin and gut swabs taken from babies on
72 NICUs from two countries (the UK and Germany) where different antiseptic regimens were in place (Sethi et
73 al., 2021). Over 1000 NAS isolates were characterised for antimicrobial susceptibility and sequenced. From
74 this collection we have analysed the population structure of *S. capitis* and compared carriage isolates with
75 those from neonatal blood cultures as well as additional isolates from healthy adult skin swabs and PJI.

76 We found that NRCS-A strains are commonly carried by uninfected neonates representing a reservoir of
77 potential infection and identified probable transmission between babies on NICU. We also identified a clade
78 closely related to NRCS-A but without an association with disease. Comparison of the NRCS-A isolates with
79 this clade ('proto NRCS-A') identified genomic and phenotypic features which may contribute to the success
80 and prevalence of this epidemic clone.

81 **Methods**

82 **Collection of isolates of *S. capitis***

83 Infants admitted to the NICUs of the Norfolk and Norwich University Hospital (Norwich, UK) or University
84 Children's Hospital (Lubeck, German) over 10-week periods in 2017 or 2018 were enrolled in this study as
85 recently described (Sethi et al., 2021). Swabs are taken routinely from babies upon admission and
86 throughout their stays in both sites for MRSA surveillance; duplicate swabs were taken for this study and
87 staphylococci isolated. In addition, isolates from positive blood, cerebrospinal fluid, urine, and wound
88 cultures were included, if taken during the study period.

89 The UK unit enrolment was between November 2017 and January 2018, and the German enrolment was
90 from January to March 2018. Amies Charcoal Swabs (Thermo Fisher Scientific) were used to isolate bacteria
91 from all infants on admission and weekly until discharge. Swabs from the ear, nose, axilla, groin and gut
92 were taken and streaked on 5% horse blood agar (Thermo Fisher), prior to incubation at 37 °C for 24 hours
93 and final identification of coagulase-negative Staphylococci after sub-culture on mannitol-salt agar (Oxoid,
94 Thermo Fisher Scientific), coagulase testing (MERCK; 75832), and/or MALDI-TOF mass spectrometry (Bruker)
95 as previously described (Sethi et al., 2021). Isolates were stored on preservation beads at -80 °C (Protect,
96 Technical Service Consultants Ltd) and in 96 deep-well plates in 20% glycerol at -40 °C. Clinical isolates of *S.*
97 *capitis* from both units which were identified by local microbiology departments during the study periods as
98 part of usual practice were also included as well as further anonymised clinical isolates taken from routine
99 blood tests taken from neonates with suspected sepsis at the NNUH NICU collected in 2018 (n=7) and
100 between June and May 2022 (n=5). In addition to isolates from neonates, a further panel of 15 *S. capitis*
101 were taken from a pre-existing Staphylococci collection isolated from adult healthy skin swabs, and clinical
102 isolates taken from adult blood cultures (where infection was suspected) and 5 recovered from PJI (Felgate
103 et al., 2021).

104 **DNA extraction**

105 Isolates were grown in 1 mL Brain Heart Infusion (BHI, MERCK) broth overnight at 37 °C. Cultures were
106 pelleted and resuspended in 100 µl 0.5 mg/mL lysostaphin (from *Staphylococcus staphylolyticus,* MERCK)
107 and incubated at 37 °C for a minimum of 1 hour. For Illumina sequencing DNA was extracted from the lysate
108 with the Quick-DNA Fungal/Bacterial 96 kit (Cambridge Bioscience), in accordance with the manufacturer's
109 guidelines. DNA was quantified using the Quant-iT™ dsDNA HS assay (ThermoFisher), and fluorescence was
110 measured on a FLUOstar Optima plate reader at 480/530 nm (excitation/emission).

111 For high molecular weight DNA, the Quick-DNA HMW MagBead Kit (Zymo) was used with a modified
112 protocol. Starting culture volume was increased to 500 µl and 50 µl of 0.5 mg/mL lysostaphin (from

113 *Staphylococcus staphylolyticus,* MERCK) was added, instead of lysozyme. Isolates were incubated at 37 °C for
114 1 hour prior to adding ProteinaseK. DNA was quantified with dsDNA HS Qubit Assay (ThermoFisher).

115 **Sequencing**

116 For Illumina sequencing genomic DNA was normalised to 5ng/µl in 10mM Tris-HCl. 0.5 µl of TB1
117 tagmentation DNA Buffer was mixed with 0.5 µl BLT, Tagment DNA Enzyme (Illumina) and 4 µl PCR grade
118 water in a master mix and 5 µl added to a chilled 96 well plate. 2 µl of normalised DNA (10 ng total) was
119 pipette mixed with the 5 µl of the tagmentation mix and heated to 55 °C for 15 minutes in a PCR block. A
120 PCR master mix was made up using 4 ul kapa2G buffer, 0.4 µl dNTP's, 0.08 µl Polymerase and 4.52 µl PCR
121 grade water, contained in the Kap2G Robust PCR kit (MERCK) per sample and 9 µl added to each well need
122 to be used in a 96-well plate. 2 µl of each P7 and P5 of Nextera XT Index Kit v2 index primers (Illumina) were
123 added to each well. Finally, the 7 µl of Tagmentation mix was added and mixed. The PCR was run with 72°C
124 for 3 minutes, 95°C for 1 minute, 14 cycles of 95°C for 10s, 55°C for 20s and 72°C for 3 minutes. Following
125 the PCR reaction, the libraries were quantified using the Promega QuantiFluor® dsDNA System and run on a
126 GloMax® Discover Microplate Reader. Libraries were pooled following quantification in equal quantities. The
127 final pool was double-SPRI size selected between 0.5 and 0.7X bead volumes using KAPA Pure Beads (Roche).
128 The final pool was quantified on a Qubit 3.0 instrument and run on a D5000 ScreenTape (Agilent) using the
129 Agilent Tapestation 4200 to calculate the final library pool molarity.

130 The pool was run at a final concentration of 1.5 pM on an Illumina Nextseq500 instrument using a Mid
131 Output Flowcell (NSQ® 500 Mid Output KT v2(300 CYS) Illumina) following the Illumina recommended
132 denaturation and loading recommendations which included a 1% PhiX spike in (PhiX Control v3 Illumina).
133 Data was uploaded to Basespace (www. basespace.illumina.com) where the raw data was converted to 8
134 FASTQ files for each sample.

135 For long read sequencing up to 400 ng of DNA was incubated with Ultra II End-prep reaction buffer and Ultra
136 II End-prep enzyme mix for end repair. The samples then had native barcodes (NB01-24) added with the
137 addition of the NEB Blunt/TA Ligase Master Mix and then the samples were heated on thermal cycler at 20
138 °C for 20 m, 65 °C for 10 m. The libraries were pooled and cleaned using AMPure XP beads, DNA was
139 quantified using dsDNA HS Qubit (ThermoFisher) and Tapestation (Aligent). For the adaptor ligation step,
140 Adapter Mix II (AMX II), NEBNext Quick Ligation Reaction Buffer (5X) and Quick T4 DNA Ligase was added to
141 the pooled library and cleaned using AMPure XP beads. The library was eluted and loaded on to a primed
142 MinION flow cell (Oxford Nanopore Technologies). Base calling (June 2022) was carried out using Guppy
143 (v6.06) (Oxford Nanopore Technologies).

144 **Genomic and Phylogenetic analysis**

145 Once generated, sequence data was processed via a series of pipelines on a Galaxy instance hosted at the
146 Quadram Institute Bioscience. FASTQ files were used to assigned a microbial classification and check for
147 contamination for each sample using Centrifuge (v0.15) (Kim et al., 2016). *S. capitis* strains were then used
148 for further analysis, isolates were assembled using SPAdes (v3.12.0) (Bankevich et al., 2012), with default
149 parameters applied, and resulting assemblies analysed for quality with QUAST (v5.0.2) (Mikheenko et al.,
150 2018). Isolates with less than X10 genomic coverage were omitted from the final collection.

151 Long read data was assembled using Flye (v2.5) (Lin et al., 2016, Kolmogorov et al., 2019) the Illumina short
152 reads were then mapped to the Flye scaffolds using minimap2 (v2.17) (Li and Durbin, 2010, Li and Durbin,
153 2009) and the sequence files were then polished with 2 rounds of pilon (v1.20.1) (Walker et al., 2014).

154 The phylogeny of the *S. capitis* isolates was determined using gene presence/absence after creating a tree
155 based on the core gene alignment. Prokka (v1.14.5) (Seemann, 2014) was used to annotate the assembled
156 contigs along with nine available *S. capitis* reference genomes (https://www.ncbi.nlm.nih.gov,
157 Supplementary Data 1). The GFF3 files were then submitted to ROARY (v3.13.0) to determine the core and
158 accessory genomes (requiring that 75% percent of isolates should carry a gene to be considered to be in the
159 core) (Page et al., 2015). A phylogenetic tree was inferred using IQTREE (v 1.6.12) (Nguyen et al., 2015) from
160 the core gene alignment output from Roary, and then visualised and annotated in iTOL (Letunic I. and Bork,
161 2019).

162 The presence of antimicrobial resistance and virulence genes were identified using ABRicate (v2.13.2, with
163 75% minimum identity, and 90% minimum coverage filters applied) (Seeman, 2016) and ARIBA (Hunt et al.,
164 2017) using the CARD database (v3.1.1) (Alcock et al., 2020).

165 To identify SNPs, FASTQ files were processed by Snippy (v4.4.3), and Snippy-core (v4.4.3) used to generate a
166 core alignment FASTA which was then analysed by snp-dist (v0.6.3) (Seemann, 2015, Seeman, 2019). The
167 reference genome used for all Snippy tools was the CR05 genome (NZ_CTEO01000001.1). The Snippy-core
168 alignment was then used to create a phylogeny based on core SNPs and run through IQTREE (Nguyen et al.,
169 2015), the resulting maximum likelihood tree was visualised using iTOL (Letunic I. and Bork, 2019).

170 Homologues of specific sequences of interest were identified using BLASTn, sequence data for the *SCCmec-*
171 *SCCcad-SCCars-SCCcop* (KF049201.1) mobile element was used as a reference to identify other similar
172 sequences in the collection using BLASTn megablast (v2.10.1; default settings)) (Camacho et al., 2009, Cock
173 et al., 2015). The NCBI protein database was searched for homologues to Nsr (CDI72769.1) and TarJ
174 (CDI72761.1) with BLASTp (Cock et al., 2015).

175 Alignment of CRISPR-Cas Type-III-A genes from different strains was assessed by taking a reference sequence
176 from *S. capitis* CR05 and creating a Snippy-core full alignment which was then submitted to ClustalW (v1.91)
177 (Larkin et al., 2007).

178 Long read sequences were compared using BLASTn pairwise alignment (NCBI, 2022) and visualised using
179 Artemis Comparison Tool (Carver et al., 2008).

180 **Antimicrobial Susceptibility Testing**

181 The susceptibility of all *S. capitis* isolates to the biocides chlorhexidine gluconate (CHX) and octenidine
182 hydrochloride (OCT) and the antibiotics, benzylpenicillin (PEN), cefotaxime (CEF), daptomycin (DAP),
183 gentamicin (GEN), fusidic Acid (FUS) and vancomycin (VAN) was determined in Mueller-Hinton agar (for
184 daptomycin, Ca^{2+} was added to a final of concentration 50 mg/L) (Sigma-Aldrich) in accordance with EUCAST
185 guidelines. Plates were inoculated with ~10^4 cells diluted from overnight cultures grown in Mueller-Hinton
186 broth (Sigma-Aldrich) using a multi-point inoculator (Denley). *Staphylococcus aureus* controls were run on all
187 the plates, ST 239 ('TW20') and NCTC 8532 ('F77') were used on the biocide plates and ATCC 29213 for the
188 antibiotic plates. The plates were incubated at 37 °C for 24 hours before minimum inhibitory concentrations
189 (MICs) were determined. MIC_{50} and MIC_{90} were determined by identifying the MIC which inhibits 50% or 90%
190 of the collection. Clinical breakpoints from EUCAST (2021) were used where applicable and cut off points for
191 CHX and OCT were set at 4 µg/mL and 2 µg/mL respectively, as defined by Htun et al. (2019). Statistical
192 analysis was performed using Graph Pad Prism (v5.04). For analysis of more than 2 groups a 1-way ANOVA
193 Kruskal-Wallis, Non-Parametric test was used.

194 **Sensitivity to pH**

195 Two randomly selected isolates from each of the Non NRCS-A, proto NRCS-A and NRCS-A groups were used
196 to test for ability to grow at pH (pH range 3.5 -10). Overnight cultures of each were used to inoculate plates
197 in duplicate (PM10 MicroPlate™ pH, Biolog, U.K) in accordance with the manufacturer's protocol and
198 respiratory activity in each sample measured over 24 hours automatically using the OmniLog reader (Biolog,
199 U.K).

200

201 **Results**

202 ***Staphylococcus capitis* were isolated from various body sites of babies on NICUs**

203 Routine MRSA swabs were taken from a total of 159 babies across their stay in NICU, *S. capitis* was isolated
204 from 55 babies (34.5 %) admitted to NICU in the UK and Germany yielding a total of 102 *S. capitis* isolates
205 (UK n=90, German n=14) from 4 different body sites (ear n=47; gut n=13; nose n=17; skin n=27). A further 12
206 isolates were from neonates with infection, 11 from blood and one from skin. A total of 15 *S. capitis* were
207 collected from adults including from prosthetic joint infection (n=3), blood (n=5) healthy skin swabs (n=6)
208 and one from an abdominal swab. All these 129 strains were sequenced and gave an average genome size of
209 2.52 Mbp with an average GC content of 32.86 %. A further 9 previously published reference genomes were
210 also included in later analysis of genomic relationships.

211 **Antiseptic susceptibility differed between isolates from different geographical sites**

212 All the isolates from the NICU CoNS collection were tested for antiseptic and antibiotic susceptibility
213 (Supplementary Data 2, Sethi et al. (2021)). The *S. capitis* isolates demonstrated greater sensitivity to
214 octenidine than chlorhexidine (MIC^{50} of 2 µg/mL and 16 µg/mL respectively, and MIC^{90} being 4 µg/mL and 32
215 µg/mL) (Figure 1). There was no significant difference found in susceptibility of isolates from different body
216 sites, but the MIC^{50} values for both octenidine and chlorhexidine in the German isolates (OCT 1 µg/mL; CHX 8
217 µg/mL) were lower than those of the UK isolates (OCT 2 µg/mL; CHX 16 µg/mL). As well as the antiseptics,
218 UK isolates had higher MIC^{50} values for gentamicin, penicillin and fusidic acid. The largest discrepancy being
219 for fusidic acid where the MIC^{50} increased from 0.625 µg/mL for the German population to 4 µg/mL in UK
220 isolates. Seven adult isolates showed hetero-resistance to daptomycin (defined as an MIC ≥ 1 µg/mL, Becker
221 et al. (2014)) but this was not seen in any neonatal isolates. No vancomycin resistance was observed in the
222 isolates with the highest MIC being 2 µg/mL, however nearly a quarter of the isolates exhibited
223 heteroresistance to vancomycin (29 in total), with the majority of these (23/29) being from NICU.

224 **Phylogenetic characterisation of *S. capitis* identified two major clades**

225 A phylogenetic tree was built using the core gene alignment output by Roary of all isolates in the panel (as
226 well as the nine available NCBI reference *S. capitis* genomes in Supplementary Data 1) then aligned with
227 IQTREE (Figure 1). Clades including NRCS-A strains were determined based on similarity to known NRCS-A
228 reference strains (CR01, 03 and 05) and by the presence of the two genes *nsr* and *tarJ,* common identifiers
229 used for this clone (Martins Simões et al., 2013). The tree showed a diversity of non-NRCS-A clones and then
230 a clonal group which all carried *nsr* and *tarJ* and included the NRCS-A strains but could be divided into two
231 further groups based on carriage of a CRISPR system.

232 **The 'non NRCS-A'** group (Figure 1, green, n=27) contained no known NRCS-A strains but did include other *S.*
233 *capitis* NCBI reference genomes and isolates from adults as well as some NICU isolates. Isolates in this group
234 tended to show a low tolerance to OCT and CHX (OCT MIC_{50} = 2 µg/mL, CHX MIC_{50} = 8 µg/mL; Table 1 and
235 fusidic acid with *fusB* being absent in all but one strain (Supplementary Data 3). Of these non NRCS-A isolates
236 12 came from the NICU (4 German, 8 UK), nine came from healthy adult skin swabs (n=5) or blood cultures
237 (n=4) and this group also included six non NRCS-A reference strains (*S. capitis* strains AYP1020, C87, QN1,
238 SK14, VCU116 and NCTC11045 (Supplementary Data 1)).

239 **The 'Proto NRCS-A'** group (denoted as such as it appears ancestrally related to the NRCS-A group and
240 contain *nsr* and *tarJ* but no CRISPR system) (Figure 1, orange, n=16) carried fewer AMR genes than the
241 NRCS-A isolates and typically lacked *fusB,* however these strains were closely related to the NRCS-A group.
242 This proto-NRCS-A clade had OCT and CHX susceptibilities lower than NRCS-A (OCT MIC_{50} = 2 µg/mL, CHX
243 MIC_{50} = 8 µg/mL: Table 1). Along with ten isolates from NICU, the remaining isolates were sourced from
244 adult PJI (n=3), blood (n=1), an abdominal swab and a healthy adult skin swab.

245 **The 'NRCS-A'** group (Figure 1, red, n=95) was the largest and contained most isolates as well as NRCS-A
246 reference strains, *S. capitis* CR01, CR03 and CR05 along with the remaining *S. capitis* isolated from the NICU.
247 No isolates from adults were found in this clade. Tolerance to OCT and CHX was marginally higher than
248 isolates from proto NRCS-A (OCT MIC_{50} = 2 µg/mL, CHX MIC_{50} = 16 µg/mL: Table 1). NRCS-A was defined by
249 isolates carrying multiple AMR genes including *blaZ* (β-lactamase)*, fusB* (fusidic acid resistance)*, AAC(6')-Ia-*
250 *APH(2")-Ia* (aminoglycoside resistance) and *mecA* (penicillin/methicillin resistance) and contained the *nsr*
251 and *tarJ* genes as well as a CRISPR-Cas Type III-A system (Figure 1and Supplementary Data 3).Multiple
252 isolates of *S. capitis* were isolated on different sampling dates from 24 separate babies (Figure 2) with the
253 remaining 40 babies only yielding a single isolate. Only 4/64 babies carried only non NRCS-A *S. capitis* strains
254 (babies 48, 58, 94 and 146, Figure 2). The remaining 60 babies carried NRCS-A isolates (Supplementary Data
255 2). Three babies (baby 8, 59, and 137) yielded *S. capitis* isolates from two of the three groups (Non NRCS-A 1
256 and NRCS-A), and one baby had two distinct isolates from the proto NRCS-A group (baby 28), and another
257 yielded one non NRCS-A and one proto NRCS-A isolate (Supplementary Data 2).

258 The number of SNPs distinguishing all 138 isolates was determined using snippy with UK NRCS-A CR05 as a
259 reference. The mean (standard deviation) number of SNPs seen between isolates in the NRCS-A, and proto
260 NRCS-A groups were 115.47 and 265 respectively (Supplementary Data 4). On average the non NRCS-A
261 isolates contained 23084.5 (3263.2) SNPs, a much higher number confirming that this clade is genetically
262 distant from the NRCS-A isolates and more diverse. The 92 NRCS-A isolates from NICU had a maximum of 31
263 snps between each other (mean aligned core genome: 2401507 bp), these isolates were only isolates from

264 the UK (Supplementary Data 4). This high degree of relatedness of isolates in the UK NICUs suggests a recent
265 common ancestor with transition across the unit and further confirms the nature of NRCS-A.

266 **Evidence for transmission within the NICU**

267 We analysed relationships between isolates taken longitudinally from babies (Figure 2), this revealed a
268 cluster of 8 isolates (209, 878, 33, 97, 191, 1048, 355, 489) differentiated by only 3 SNPS, (Supplementary
269 Data 5) recovered between over 70 days, from six different babies (Figure 2) suggesting transmission within
270 the NICU environment and persistence of isolates over time. The total number of SNPs between all NRCS-A
271 isolates was only 37. This indicates that very similar closely related isolates were present in the UK NICUs
272 and they remain present for years with very little genomic change.

273 **Differences distinguishing clades**

274 The collection was analysed by Roary, (Page et al., 2015) to identify genes that were either present or absent
275 in the clades, 'Scoary' was then used to calculate statistical associations between the presence and absence
276 of genes, clade membership and a series of phenotypes (Brynildsrud et al., 2016). Notably the genes being
277 most significantly associated with the NRCS-A clade were the CRISPR genes, all NRCS-A isolates harboured a
278 complete CRISPR-Cas Type-III-A system. None of the closely related proto NRCS-A isolates harboured any
279 CRISPR Cas Type-III-A genes. These Cas Type-III-A genes are inserted in the *SCCmec-SCCcad/ars/cop* element
280 (Figure 3). Two virulence genes *paaZ* and *ugpQ,*along with *dut* are known to be closely located to *mecA,* and
281 were also strongly associated with being present in the NRCS-A isolates (Datta et al., 2021, Westberg et al.,
282 2022).

283 Scoary analysis also identified groups of other genes significantly associated with the NRCS-A isolates. Many
284 of these genes were annotated as being of unknown function and clustered together in the genomes.
285 Further analysis of these genes, using Blastn identified several as being putative phage terminases which are
286 inserted in-between *yfnK* and *murI,* immediately downstream from *frdA, uvrC* and *mutS.* Scoary also
287 identified *mcrC* in NRCS-A isolates which is involved in regulation of degrading methylated bacteriophage
288 DNA (Nirwan et al., 2019) (Table 2, Supplementary Data 6).

289 Previous research by Martins Simões et al. (2013) suggested the presence of *nsr* and *tarJ* as a defining
290 characteristic of the NRCS-A clone, and both these genes are present in both NRCS-A and proto NRCS-A
291 isolates. The *tarLIJ* locus encodes a Ribulose-5-phosphate reductase which are involved in teichoic acid
292 biosynthesis (Tevell et al., 2020, Martins Simões et al., 2013). These were significantly associated with the
293 NRCS-A group, parts of the operon were found in Non NRCS-A but were usually incomplete (Figure 1, Table
294 2). All NRCS-A and proto NRCS-A isolates had *tarJ* compared to only 3.7% of non NRCS-A isolates (Figure 1).
295 The *nsr* gene associated with nisin resistance was identified in both NRCS-A and proto NRCS-A isolates, and

296 *kdpDC* was also significantly over-represented in these groups which encodes a potassium pump encoded
297 close to *nsr* in the genome (Martins Simões et al., 2013).

298 There was a significant increase in the presence of genes involved in metal transport in the NRCS-A group
299 compared to the others (Table 3, Supplementary Data 6). ABC permeases *cnt ABCDEFKL, nikC* and *oppDF*
300 were all identified and are involved in the acquisition of Zn and Ni (Grim et al., 2017). Further genes involved
301 in metal detoxification were also seen in NRCS-A, the *copB, copAZ, arsBC* and *cadC* systems were over-
302 represented in this clade. These have all been previously identified as part of an SCC*mec* element (*SCCmec-*
303 *SCCcad/ars/cop*) also containing the CRISPR-Cas Type III-A system in NCRS-A isolates. As well as genes
304 associated with this element, the NRCS-A isolates could also be distinguished from the proto-NRCS-A clade
305 by the presence of *mntH* (Table 3, Supplementary Data 6).

306 Previously it has been suggested that NRCS-A isolates are adapted to survive in both the gut and on the skin,
307 two environments where pH differs. We observed that growth of both proto NRCS-A and NRCS-A isolates at
308 lower pH was higher compared to non NRCS-A isolates (Figure 4). Growth at pH 6 and pH 5.5 was also
309 marginally higher compared to pH 7 in both the NRCS-A and proto NRCS-A isolates (Figure 4).

310 To compare conservation of the *SCCmec* element seen in all the isolates, the S*CCmec-SCC-cad/ars/cop*
311 sequence of CR01 (GenBank KF049201.1) was compared to all the *S. capitis* isolates using snippy-core and
312 snp-dist (Seemann, 2015, Seeman, 2019). All isolates and references except for VCUII6 aligned to the
313 S*CCmec-SCC-cad/ars/cop* reference. The NRCS-A isolates, on average, had 12.3 ± 0.5 SNPs, which increased
314 to 64.4 ± 11.1 in non NRCS-A and 190.9 ± 22.5 in proto NRCS-A isolates. The higher divergence in the proto
315 NRCS-A group is surprising given its closer relationship to the NRCS-A group according to the core genome
316 phylogeny.

317 Further analysis of the CRISPR-Cas Type III-A system showed that the genes were highly conserved when
318 aligned. In all isolates it was possible to identify direct repeat (DR) sequences (beginning with GATAACT), and
319 there were three different DRs present in the isolates as previously observed in CR01 Cao et al. (2016). In a
320 full SNP ClustalW alignment DR5 (4 times) and DR6 (3 times) were found before the Cas genes, and then two
321 repeats of DR8 towards the end of the alignment after the CRISPR genes (Cao et al., 2016).

322 **Carriage of AMR genes varied between non NRCS-A and NRCS-A**

323 All isolates contained *lmrS, norA, arlR* and *dfrC*, and all but one isolate contained *mgrA*. NRCS-A was defined
324 by the additional presence of *blaZ, mecA, ACC(6')-le(APH)(2')-la* and *fusB* in the majority of isolates whereas
325 proto NRCS-A had a smaller number of AMR genes which were interspersed across the clade without a
326 consistent pattern (Figure 1, Supplementary Data 3). Analysis of the pangenomes with Scoary was used to
327 identify genes correlating with susceptibility to different antimicrobials. Unsurprisingly *mecA* was strongly

328 associated with high cefotaxime MICs (4 µg/mL, Supplementary Data 6). Carriage of *blaZ* was also associated
329 with penicillin resistance (≥1 µg/mL, P= 0.005), however CRISPR genes (P= 0.002) and other genes commonly
330 found on the S*CCmec-SCC-cad/ars/cop* MGE were more significant (Table 4). The *qac* family of genes has
331 previously been implicated in tolerance to antiseptics, *qacA* was detected but only present in 22/138 (16 %)
332 isolates and there was no correlation with the presence of *qacA* and CHX tolerance. Carriage of *qacA* was
333 only observed in 16.25% of isolates with high chlorhexidine MICs ≥16 µg/mL (Figure 1). For isolates that had
334 an MIC to chlorhexidine of ≥16 µg/mL the genes mostly associated with this tolerance were the CRISPR-Cas
335 Type III-A, Supplementary Data 6). This is a marker of NRCS-A isolates which had significantly higher
336 chlorhexidine MICs (Figure 5) although there was no obvious genetic basis for this. Scoary was unable to
337 identify any significant genes associated with octenidine susceptibility.

338 The classic antibiogram for NRCS-A isolates includes being resistant to fusidic acid (PHE, 2021), with the
339 clinical breakpoint being ≥0.5 µg/mL for all CoNS (EUCAST, 2021). Based on this criterion 79% of our
340 collection tested were clinically resistant and carriage of *fusB* was seen in 78.75 % of these resistant isolates,
341 leaving 17 isolates with no known mechanism of fusidic acid resistance. The presence of *fusB* was mainly
342 observed in NRCS-A, where there was a small increase in tolerance to fusidic acid, with the mean MIC being
343 2.95 (SD: 0.155) µg/mL, higher than non NRCS-A (1.40, SD: 0.301 µg/mL). The UK isolates had a higher
344 median FUS MIC (4 µg/mL) than the German isolates (1.5 µg/mL) (P = <0.01). Penicillin resistance encoded
345 by *mecA* was seen in 86% of the isolates with an MIC ≥ 2 µg/mL (Supplementary Data 2 and 3), and carriage
346 of *ACC(6')-Ia-APH(2")-Ia* was seen in 73% of isolates with an MIC ≥1 µg/mL of gentamicin. No genes were
347 associated with ciprofloxacin resistance although the main mechanism of resistance to this agent is target
348 site mutation within *gyrA* rather than the presence of a gene.

349 *S. capitis* NRCS-A are often referred to as demonstrating hetero-resistance to vancomycin, indicated by a
350 MIC of 2 µg/mL (Satola et al., 2011). Despite 23.5% of the isolates having an MIC of 2 µg/mL there was no
351 presence of *vanA* apart from in one isolate (with an MIC of 1 µg/mL) or any other significant genes
352 associated with vancomycin resistance.

353

354 **Discussion**

355 Even with the increased focus on their prevention, nosocomial infections remain a major cause of disease
356 and death in hospitals. Transmission of bacterial pathogens can occur via multiple routes and vectors with
357 both health care workers and the environment sources of infection for many pathogens such as
358 *Staphylococcus aureus, Pseudomonas aeruginosa* and Enterobacteriaceae (Risso et al., 2019, Götting et al.,
359 2020). The effective adaption of the NRCS-A clone to the NICU environment is well established, though the
360 reasons for this remain unclear. One suggestion is that NRCS-A isolates are adapted to survival in the gut
361 which provides an additional reservoir to the skin and may allow persistent colonisation, even when skin
362 organisms are lost during antisepsis (Butin et al., 2017). Carriage of the *nsr* gene responsible for nisin
363 resistance has been proposed to aid survival in the gut where this antimicrobial peptide is produced (Martins
364 Simões et al., 2013). In this study we documented carriage of NRCS-A on both the skin of neonates and in the
365 gut, and this was much more common than for other groups of *S. capitis* (Figure 1). We did observe that the
366 *nsr* gene is present in NRCS-A isolates but not in more distantly related strains. Interestingly we identified a
367 group of isolates closely related to NCRS-A, the 'proto NRCS-A' strains which did carry *nsr* but which were
368 isolated from the gut less often (Figure 1). It was also observed that the proto NRCS-A and NRCS-A isolates,
369 which possess *nsr* and *tarJ,* had increased growth in pH 6-5.5 cultures (Figure 4), analogous to their niche in
370 the gastrointestinal tract.

371 *Metal acquisition and survival*

372 Analysis of the pangenomes of each group identified other genes that may aid the survival of the NRCS-A in
373 the NICU. In the NRCS-A isolates there was a marked increase in genes associated with metal chelation
374 (Table 2), availability of many metals is limited *in vivo* and in the gut metals are precious commodities. Metal
375 chelators can also influence virulence, for example, the nickel/cobalt transporter *nixA* in *S. aureus* has been
376 implicated in an increase in virulence in UTI and kidney infection and is required for urease activity in mice
377 (Remy et al., 2013). Other metal related genes found in NRCS-A were *mntH*, a metal transporter found to
378 minimise impact of Mn and Zn starvation (Kehl-Fie et al., 2013), and *cntABCDEF* which functions with
379 Staphylopine, StP (CntKLM) a staphylococcal zincophore involved in Zn acquisition which can also bind to Cu,
380 Co and Ni (Grim et al., 2017, Song et al., 2018). These high affinity chelators and zincophores have been
381 shown to be able to outcompete human calprotectin (a Zn chelator excreted by neutrophils) to evade
382 nutritional immunity. The presence of *cntABCDEF cntKLM, nixA* and *mntH* may indicate that even in
383 nutritionally deprived environments, the NRCS-A isolates are able to acquire essential metal ions and survive
384 in a gut environment. Similarly, the presence of *copA, cad,* and *ars,* encoded within the *SCCmec-*
385 *SCCcad/ars/cop* element in NRCS-A provide defence against toxic metals by encoding efflux systems.
386 Together these data suggest that an enhanced ability to scavenge and survive metal exposure may be crucial

387 for the success of NRCS-A and supports the theory that gut colonisation is a key strategy exploited by this
388 clone.

389 *Phage defence*

390 If NRCS-A has developed a lifestyle which includes ability to colonise the gut then it also needs to adapt to
391 attack from phages, which are prevalent in this environment. In *Escherichia coli* the *mcrBC* genes provide
392 protection from phages and McrC activates McrB to degrade methylated bacteriophage DNA (Nirwan et al.,
393 2019). MrcC was seen in our collection but *mcrB* was not detected and it is unclear what impact *mcrC* alone
394 may have. Other mechanisms of phage defence observed in the NRCS-A isolates were the CRISPR-associated
395 genes (Cas), used in defence against MGEs, viruses and plasmids (Tamulaitis et al., 2017, Rossi et al., 2017).
396 CRISPR-Cas systems show low abundance in most Non-aureus Staphylococci although they have been
397 documented in the genomes of *S. aureus* strains as well as in *S. epidermidis, S. schleiferi, S. haemolyticus, S.*
398 *lugdunensis*. Carriage of a CRISPR-Cas system is a known feature of NRCS-A *S capitis* and CRISPR-Type III-A
399 Cas genes were identified in all NRCS-A isolates. This was the main defining feature differentiating the proto
400 NRCS-A and the NRCS-A clades, however when this system was acquired by NCRS-A remains unclear. The
401 direct repeats identified are similar to that as previously seen in CR01 and CR03 which both contain the
402 conserved CCCC and GGGG motifs which are thought to form hairpin structures (Rossi et al., 2017). The
403 highly conserved regions suggest that a common ancestor is responsible for the acquisition of the CRISPR-
404 Cas Type-III-A genes.

405 *Antiseptic tolerance*

406 One defining feature of the NRCS-A clade was increased tolerance of chlorhexidine (Figure 5), this was not
407 associated with carriage of *qac* genes, and the mechanism remains unclear. This increased ability to survive
408 chlorhexidine exposure may allow both survival of skin antisepsis but also environmental decontamination
409 where chlorhexidine is a common part of cleaning and disinfection routines for incubators and medical
410 equipment. There was no elevation in tolerance to octenidine, which is the main alternative for antisepsis in
411 neonates (Sethi et al., 2021).

412 *Stability of NRCS-A*

413 The NRCS-A isolates compared here were very similar including those separated by geography (UK and
414 German isolates) and time (reference genomes spanning years in isolation) (Figure 2), and there were no
415 more than 37 SNPs separating strains in the core genome. We provide evidence for transfer between babies
416 on the NICU (Figure 2), studies identifying NRCS-A in the general environment and on different surfaces or
417 medical implements following clusters of LOS NRCS-A positive cases have suggested a role for the
418 environment in transmission The isolates from carriage and the 10 from neonatal blood cultures were highly

419 similar (Figure 1). This supports the idea that carriage acts as a reservoir for infection but clearly carriage by
420 neonates in a nosocomial setting does not usually result in infection.

421 **Conclusions**

422 We have identified that carriage of the NRCS-A clone is abundant on the skin and gut of uninfected neonates
423 and that they are likely to be transferred within NICUs. NRCS-A isolates separated in time and space showed
424 little genetic variation and carriage isolates were indistinguishable to those from blood culture, suggesting
425 carriage can be a precursor to infection. We identified a closely related proto-NRCS-A clade which was less
426 associated with gut carriage, did not possess the CRISPR-Cas III-A system, demonstrated lower antimicrobial
427 resistance and chlorhexidine tolerance and carried fewer metal acquisition or detoxification genes. Our data
428 supports the idea that gut colonisation is a key survival strategy of NRCS-A and expands our understanding
429 of the likely mechanisms employed by this clone to both survive on skin, in the environment and in the gut.
430 This opens the possibility to develop a probiotic approach to hinder colonisation of NCRS-A based upon
431 nutritional immunity where strains that sequester essential metals may prove beneficial to the infant gut.
432 Recent deployment of a probiotic product into the NNUH NICU has been used to reduce incidence of
433 necrotising enterocolitis with success and was also associated with reduced episodes of infection with CoNS
434 ((Robertson et al., 2020). More work can help develop strategies to identify reservoirs and transmission
435 routes of NRCS-A and to eradicate carriage from neonates to prevent infection which can have serious
436 consequences.

Funding

This work was supported by an award from the Biotechnology and Biological Sciences Research Council (BB/T014644/1). For the purpose of open access, the author has applied a Creative Commons Attribution (CC BY) licence to any Author Accepted Manuscript version arising from this submission.

Data accessibility

Sequence data for all isolates have been uploaded to the SRA under Project number PRJNA751027

Conflict of interest

There are no conflicts of interest

Ethics

The collection of weekly neonatal skin swabs in 2017-18 received prior approval as a surveillance study by the Research and Development Manager of the Norfolk and Norwich University Hospitals NHS Foundation Trust and did not require formal research ethics review. In Germany, the study was reviewed and approved as a surveillance study by the University of Lubeck Hospital ethics committee (reference AZ 15-034, amendment 01/2018). Clinical isolates were provided under NHS Research Ethics Committee approval to the Norwich Biorepository which banks blood, solid tissue and bacterial isolates from the NNUH and research institutes on the Norwich Research Park, including the University of East Anglia, and makes these available to the research community.

Author Contributions

Dheeraj Sethi, Heather Felgate, Paul Clarke and Mark Webber were involved in study conception and design. Collection and processing of the Staphylococci library was carried out by Dheeraj Sethi. Kirstin Faust, Cemsid Kiy, Christoph Härtel and Jan Rupp were involved in the isolate collection from the German NICU. Heather Felgate, Dheeraj Sethi, Rebecca Clifford and Rachel Dean were involved with sequencing strains. Heather Felgate carried out phenotyping, data analysis and genotyping of the collection, as well as writing the first draft of the manuscript. Catherine Tremlett provided isolates from LOS and provided input on the manuscript. Heather Felgate, Christoph Härtel, Cemsid Ki, John Wain, Gemma Langridge, Paul Clarke, Andrew Page, Mark A Webber were all involved in the production of the manuscript and scientific input.

Acknowledgements

We would like to acknowledge the nurses within NICUs in Lubeck and Norwich who helped with isolation of S. *capitis* from neonates and the microbiology lab staff at the NNUH and Lubeck hospital who also helped process and save isolates.

467 **References**

468 ALCOCK, B., RAPHENYA, A., LAU, T., TSANG, K., BOUCHARD, M., EDALATMAND, A., HUYNH, W., NGUYEN, A.,
469 CHENG, A., LIU, S., MIN, S., MIROSHNICHENKO, A., TRAN, H., WERFALLI, R., NASIR, J., OLONI, M.,
470 SPEICHER, D., FLORESCU, A., SINGH, B., FALTYN, M., HERNANDEZ-KOUTOUCHEVA, A., SHARMA, A.,
471 BORDELEAU, E., PAWLOWSKI, A., ZUBYK, H., DOOLEY, D., GRIFFITHS, E., MAGUIRE, F., WINSOR, G.,
472 BEIKO, R., BRINKMAN, F., HSIAO, W., DOMSELAAR, G. & MCARTHUR, A. 2020. CARD 2020: antibiotic
473 resistome surveillance with the Comprehensive Antibiotic Resistance Database. *Nucleic Acids*
474 *Research,* 48**,** D517-D525.

475 BANKEVICH, A., NURK, S., ANTIPOV, D., GUREVICH, A., DVORKIN, M., KULIKOV, A., LESIN, V., NIKOLENKO, S.,
476 PHAM, S., PRJIBELSKI, A., PYSHKIN, A., SIROTKIN, A., VYAHHI, N., TESLER, G., ALEKSEYEV, M. & PA., P.
477 2012. SPAdes: A New Genome Assembly Algorithm and Its Applications to Single-Cell Sequencing.
478 *Journal of Computational Biology,* 19.

479 BECKER, K., BOTH, A., WEIßELBERG, S., HEILMANN, C. & ROHDE, H. 2020. Emergence of coagulase-negative
480 staphylococci. *Expert Review of Anti-infective Therapy,* 18**,** 349-366.

481 BECKER, K., HEILMANN, C. & PETERS, G. 2014. Coagulase-Negative Staphylococci. *Clinical Microbiology*
482 *Reviews,* 27**,** 870-926.

483 BEN SAID, M., HAYS, S., BONFILS, M., JOURDES, E., RASIGADE, J. P., LAURENT, F. & PICAUD, J. C. 2016. Late-
484 onset sepsis due to *Staphylococcus capitis* 'neonatalis' in low-birthweight infants: a new entity?
485 *Journal of Hospital Infection,* 94**,** 95-98.

486 BENTLIN, M., DE SOUZA, R. & MS., L. 2010. Late-onset Sepsis: Epidemiology, Evaluation, and Outcome.
487 *NeoReviews,* 11**,** e426-e435.

488 BRYNILDSRUD, O., BOHLIN, J., SCHEFFER, L. & ELDHOLM, V. 2016. Rapid scoring of genes in microbial pan-
489 genome-wide association studies with Scoary. *Genome Biol.,* 17.

490 BUTIN, M., DUMONT, Y., MONTEIX, A., RAPHARD, A., ROQUES, C., MARTINS SIMOES, P., PICAUD, J.-C. &
491 LAURENT, F. 2019. Sources and reservoirs of Staphylococcus capitis NRCS-A inside a NICU.
492 *Antimicrobial Resistance & Infection Control,* 8**,** 157.

493 BUTIN, M., MARTINS-SIMÕES, P., RASIGADE, J.-P., PICAUD, J.-C. & LAURENT, F. 2017. Worldwide Endemicity
494 of a Multidrug-Resistant *Staphylococcus capitis* Clone Involved in Neonatal Sepsis. *Emerging*
495 *infectious diseases,* 23**,** 538-539.

496 CAMACHO, C., COULOURIS, G., AVAGYAN, V., MA, N., PAPADOPOULOS, J., BEALER, K. & MADDEN, T. L. 2009.
497 BLAST+: architecture and applications. *BMC Bioinformatics,* 10**,** 421.

498 CAO, L., GAO, C.-H., ZHU, J., ZHAO, L., WU, Q., LI, M. & SUN, B. 2016. Identification and functional study of
499 type III-A CRISPR-Cas systems in clinical isolates of Staphylococcus aureus. *International Journal of*
500 *Medical Microbiology,* 306**,** 686-696.

501 CARTER, G., USSHER, J., DA SILVA, A., BAINES, S., HEFFERNAN, H., RILEY, T., BROADBENT, R., VAN DER
502 LINDEN, A., LEE, J., MONK, I., STINEAR, T., HOWDEN, B. & WILLIAMSON, D. 2018. Genomic Analysis
503 of Multiresistant *Staphylococcus capitis* Associated with Neonatal Sepsis. *Antimicrobial Agents and*
504 *Chemotherapy,* 62**,** e00898-18.
505 CARVER, T., BERRIMAN, M., TIVEY, A., PATEL, C., BÖHME, U., BARRELL, B. G., PARKHILL, J. & RAJANDREAM,
506 M.-A. 2008. Artemis and ACT: viewing, annotating and comparing sequences stored in a relational
507 database. *Bioinformatics,* 24**,** 2672-2676.
508 COCK, P. J. A., CHILTON, J. M., GRÜNING, B., JOHNSON, B. E. & SORANZO, N. 2015. NCBI BLAST+ integrated
509 into Galaxy. *GigaScience,* 4.
510 DATTA, M. S., YELIN, I., HOCHWALD, O., KASSIS, I., BORENSTEIN-LEVIN, L., KUGELMAN, A. & KISHONY, R.
511 2021. Rapid methicillin resistance diversification in Staphylococcus epidermidis colonizing human
512 neonates. *Nature Communications,* 12**,** 6062.
513 DONG, Y. & SPEER, C. 2014. The role of Staphylococcus epidermidis in neonatal sepsis: Guarding angel or
514 pathogenic devil? . *Int J Med Microbiol,* 304**,** 513-20.
515 DU, X., LARSEN, J., LI, M., WALTER, A., SLAVETINSKY, C., BOTH, A., SANCHEZ CARBALLO, P., STEGGER, M.,
516 LEHMANN, E., LIU, Y., LIU, J., SLAVETINSKY, J., DUDA, K., KRISMER, B., HEILBRONNER, S.,
517 WEIDENMAIER, C., MAYER, C., ROHDE, H., WINSTEL, V. & PESCHEL, A. 2021. Staphylococcus
518 epidermidis clones express Staphylococcus aureus-type wall teichoic acid to shift from a commensal
519 to pathogen lifestyle. *Nature Microbiology*.
520 EUCAST 2021. European Committee on Antimicrobial Susceptibility Testing.
521 FELGATE, H., CROSSMAN, L. C., GRAY, E., CLIFFORD, R., CORREIA, A., DEAN, R., WAIN, J. & LANGRIDGE, G. C.
522 2021. Known mechanisms account for less than half of antimicrobial resistance in a diverse
523 collection of non-aureus staphylococci. *bioRxiv***,** 2021.06.22.449369.
524 GÖTTING, T., REUTER, S., JONAS, D., HENTSCHEL, R., HENNEKE, P., KLOTZ, D., HOCK, S., WOLKEWITZ, M.,
525 BLÜMEL, B., HÄCKER, G., GRUNDMANN, H. & MUTTERS, N. 2020. Protocol for a prospective cohort
526 study: Prevention of Transmissions by Effective Colonisation Tracking in Neonates (PROTECT-Neo).
527 *BMJ open,* 10**,** e034068-e034068.
528 GRIM, K. P., SAN FRANCISCO, B., RADIN, J. N., BRAZEL, E. B., KELLIHER, J. L., PÁRRAGA SOLÓRZANO, P. K.,
529 KIM, P. C., MCDEVITT, C. A. & KEHL-FIE, T. E. 2017. The Metallophore Staphylopine Enables
530 Staphylococcus aureus To Compete with the Host for Zinc and Overcome Nutritional Immunity.
531 *mBio,* 8.
532 HARVEY, E. J., ASHIRU-OREDOPE, D., HILL, L. F., DEMIRJIAN, A. & TEAM., U. K. H. S. A. S. C. I. M. 2022. Need
533 for standardized vancomycin dosing for coagulase-negative staphylococci in hospitalized infants. *Clin*
534 *Microbiol Infect*.

535 HTUN, H. L., HON, P. Y., HOLDEN, M. T. G., ANG, B. & CHOW, A. 2019. Chlorhexidine and octenidine use,
536 carriage of *qac* genes, and reduced antiseptic susceptibility in methicillin-resistant *Staphylococcus*
537 *aureus* isolates from a healthcare network. *Clinical Microbiology and Infection,* 25**,** 1154.e1-1154.e7.
538 HUNT, M., MATHER, A., SÁNCHEZ-BUSÓ, L., PAGE, A., PARKHILL, J., KEANE, J. & HARRIS, S. 2017. ARIBA: rapid
539 antimicrobial resistance genotyping directly from sequencing reads. *Microbial Genomics,* 3.
540 KEHL-FIE, T. E., ZHANG, Y., MOORE, J. L., FARRAND, A. J., HOOD, M. I., RATHI, S., CHAZIN, W. J., CAPRIOLI, R.
541 M. & SKAAR, E. P. 2013. MntABC and MntH contribute to systemic Staphylococcus aureus infection
542 by competing with calprotectin for nutrient manganese. *Infection and immunity,* 81**,** 3395-3405.
543 KIM, D., SONG, L., BREITWIESER, F. & SALZBERG, S. 2016. Centrifuge: rapid and sensitive classification of
544 metagenomic sequences. *Genome research,* 26**,** 1721-1729.
545 KOLMOGOROV, M., YUAN, J., LIN, Y. & PEVZNER, P. 2019. Assembly of long, error-prone reads using repeat
546 graphs. *Nature Biotechnology,* 37**,** 540-546.
547 LARKIN, M. A., BLACKSHIELDS, G., BROWN, N. P., CHENNA, R., MCGETTIGAN, P. A., MCWILLIAM, H.,
548 VALENTIN, F., WALLACE, I. M., WILM, A., LOPEZ, R., THOMPSON, J. D., GIBSON, T. J. & HIGGINS, D. G.
549 2007. Clustal W and Clustal X version 2.0. *Bioinformatics,* 23**,** 2947-2948.
550 LEMRISS, H., MARTINS SIMÕES, P., LEMRISS, S., BUTIN, M., IBRAHIMI, A., EL KABBAJ, S., RASIGADE, J. &
551 LAURENT, F. 2014. Non-contiguous finished genome sequence of Staphylococcus capitis CR01
552 (pulsetype NRCS-A). *Standards in genomic sciences,* 9**,** 1118-1127.
553 LEPAINTEUR, M., ROYER, G., BOURREL, A. S., ROMAIN, O., DUPORT, C., DOUCET-POPULAIRE, F. &
554 DECOUSSER, J. W. 2013. Prevalence of resistance to antiseptics and mupirocin among invasive
555 coagulase-negative staphylococci from very preterm neonates in NICU: the creeping threat? *J Hosp*
556 *Infect,* 83**,** 333-6.
557 LETUNIC I. & BORK, P. 2019. *Tree Of Life v4.4.2* [Online]. Available: https://itol.embl.de/ [Accessed 2019].
558 LI, H. & DURBIN, R. 2009. Fast and accurate short read alignment with Burrows–Wheeler transform.
559 *Bioinformatics,* 25**,** 1754-1760.
560 LI, H. & DURBIN, R. 2010. Fast and accurate long-read alignment with Burrows–Wheeler transform.
561 *Bioinformatics,* 26**,** 589-595.
562 LIN, Y., YUAN, J., KOLMOGOROV, M., SHEN, M., CHAISSON, M. & PEVZNER, P. 2016. Assembly of long error-
563 prone reads using de Bruijn graphs. *Proceedings of the National Academy of Sciences,* 113**,** E8396-
564 E8405.
565 MAKHOUL, I., SUJOV, P., SMOLKIN, T., LUSKY, A. & REICHMAN, B. 2005. Pathogen-Specific Early Mortality in
566 Very Low Birth Weight Infants with Late-Onset Sepsis: A National Survey. . *Clin Infect Dis,* 40**,** 218-24.
567 MARTINS SIMÕES, P., RASIGADE, J. P., LEMRISS, H., BUTIN, M., GINEVRA, C., LEMRISS, S., GOERING, R. V.,
568 IBRAHIMI, A., PICAUD, J. C., EL KABBAJ, S., VANDENESCH, F. & LAURENT, F. 2013. Characterization of

569 a novel composite staphylococcal cassette chromosome mec (SCCmec-SCCcad/ars/cop) in the
570 neonatal sepsis-associated *Staphylococcus capitis* pulsotype NRCS-A. *Antimicrobial agents and*
571 *chemotherapy,* 57**,** 6354-6357.
572 MIKHEENKO, A., PRJIBELSKI, A., SAVELIEV, V., ANTIPOV, D. & GUREVICH, A. 2018. Versatile genome assembly
573 evaluation with QUAST-LG. *Bioinformatics.* 5.0.2 ed.
574 NCBI, N. C. F. B. I. 2022. *The Basic Local Alignment Search Tool (BLAST)* [Online]. Available:
575 https://blast.ncbi.nlm.nih.gov/Blast.cgi [Accessed 2022].
576 NGUYEN, L.-T., SCHMIDT, H., VON HAESELER, A. & MINH, B. 2015. IQ-TREE: a fast and effective stochastic
577 algorithm for estimating maximum-likelihood phylogenies. *Molecular biology and evolution,* 32**,** 268-
578 274.
579 NIRWAN, N., ITOH, Y., SINGH, P., BANDYOPADHYAY, S., VINOTHKUMAR, K. R., AMUNTS, A. & SAIKRISHNAN,
580 K. 2019. Structure-based mechanism for activation of the AAA+ GTPase McrB by the endonuclease
581 McrC. *Nature Communications,* 10**,** 3058.
582 PAGE, A. J., CUMMINS, C., HUNT, M., WONG, V., REUTER, S., HOLDEN, M., FOOKES, M., FALUSH, D., KEANE, J.
583 & PARKHILL, J. 2015. Roary: Rapid large-scale prokaryote pan genome analysis. *Bioinformatics,* 31**,**
584 3691-3.
585 PHE. 2021. *Briefing Note 0 2021/005 Increased incidence of detections of Staphylococcus capitis in neonatal*
586 *clinical samples* [Online]. Public Health England. Available: https://hubble-live-
587 assets.s3.amazonaws.com/bapm/attachment/file/411/Increased_incidence_of_detections_of_Stap
588 hylococcus_capitis_in_neonates.pdf [Accessed April 2021].
589 RASIGADE, J. P., RAULIN, O., PICAUD, J. C., TELLINI, C., BES, M., GRANDO, J., BEN SAÏD, M., CLARIS, O.,
590 ETIENNE, J., TIGAUD, S. & LAURENT, F. 2012. Methicillin-resistant Staphylococcus capitis with
591 reduced vancomycin susceptibility causes late-onset sepsis in intensive care neonates. *PLoS One,* 7**,**
592 e31548.
593 REMY, L., CARRIÈRE, M., DERRÉ-BOBILLOT, A., MARTINI, C., SANGUINETTI, M. & BOREZÉE-DURANT, E. 2013.
594 The Staphylococcus aureus Opp1 ABC transporter imports nickel and cobalt in zinc-depleted
595 conditions and contributes to virulence. *Molecular Microbiology,* 87**,** 730-743.
596 RISSO, F., MINGHETTI, D., MARIANI, M., PARODI, A., LA MASA, D., CASTAGNOLA, E. & RAMENGHI, L. A. 2019.
597 Behaviours monitoring and infection control in neonatal intensive care unit: how to improve
598 ourselves? *J. Prev Med. Hyg.,* 60**,** E226-E228.
599 ROBERTSON, C., SAVVA, G., CLAPUCI, R., JONES, J., MAIMOUNI, H., BROWN, E., MINOCHA, A., HALL, L. &
600 CLARKE, P. 2020. Incidence of necrotising enterocolitis before and after introducing routine
601 prophylac *Lactobacillus* and *Bifidobacterium* probiotics. *Archives of Disease in Childhood - Fetal and*
602 *Neonatal Edition,* 105**,** 380.

603 ROSSI, C. C., SOUZA-SILVA, T., ARAÚJO-ALVES, A. & GIAMBIAGI-DEMARVAL, M. 2017. CRISPR-Cas Systems
604 Features and the Gene-Reservoir Role of Coagulase-Negative Staphylococci. *Frontiers in*
605 *Microbiology,* 8.
606 SATOLA, S. W., FARLEY, M. M., ANDERSON, K. F. & PATEL, J. B. 2011. Comparison of detection methods for
607 heteroresistant vancomycin-intermediate Staphylococcus aureus, with the population analysis
608 profile method as the reference method. *J Clin Microbiol,* 49**,** 177-83.
609 SEEMAN, T. 2016. ABRicate: mass screening of contigs for antiobiotic resistance genes. Github.
610 SEEMAN, T. 2019. snp-dists. GitHub repository: GitHub.
611 SEEMANN, T. 2014. Prokka: rapid prokaryotic genome annotation. *Bioinformatics,* 15**,** 2068-9.
612 SEEMANN, T. 2015. snippy: fast bacterial variant calling from NGS reads.
613 SETHI, D. K., FELGATE, H., DIAZ, M., FAUST, K., KIY, C., CLARKE, P., HÄRTEL, C., RUPP, J. & WEBBER, M. A.
614 2021. Chlorhexidine gluconate usage is associated with antiseptic tolerance in staphylococci from
615 the neonatal intensive care unit. *JAC Antimicrob Resist,* 3**,** dlab173.
616 SONG, L., ZHANG, Y., CHEN, W., GU, T., ZHANG, S.-Y. & JI, Q. 2018. Mechanistic insights into staphylopine-
617 mediated metal acquisition. *Proceedings of the National Academy of Sciences,* 115**,** 3942.
618 TAMULAITIS, G., VENCLOVAS, Č. & SIKSNYS, V. 2017. Type III CRISPR-Cas Immunity: Major Differences
619 Brushed Aside. *Trends in Microbiology,* 25**,** 49-61.
620 TEVELL, S., BAIG, S., HELLMARK, B., MARTINS SIMOES, P., WIRTH, T., BUTIN, M., NILSDOTTER-
621 AUGUSTINSSON, Å., SÖDERQUIST, B. & STEGGER, M. 2020. Presence of the neonatal Staphylococcus
622 capitis outbreak clone (NRCS-A) in prosthetic joint infections. *Scientific Reports,* 10**,** 22389.
623 WALKER, B., ABEEL, T., SHEA, T., PRIEST, M., ABOUELLIEL, A., SAKTHIKUMAR, S., CUOMO, C., ZENG, Q.,
624 WORTMAN, J., YOUNG, S. & EARL, A. 2014. Pilon: An Integrated Tool for Comprehensive Microbial
625 Variant Detection and Genome Assembly Improvement. *PLOS ONE,* 9**,** e112963.
626 WESTBERG, R., STEGGER, M. & SÖDERQUIST, B. 2022. Molecular Epidemiology of Neonatal-Associated
627 *Staphylococcus haemolyticus* Reveals Endemic Outbreak. *Microbiology Spectrum***,** e02452-22.
628 WIRTH, T., BERGOT, M., RASIGADE, J.-P., PICHON, B., BARBIER, M., MARTINS-SIMOES, P., JACOB, L., PIKE, R.,
629 TISSIERES, P., PICAUD, J.-C., KEARNS, A., SUPPLY, P., BUTIN, M., LAURENT, F., ADAMKOVA, V.,
630 BARKHAM, T., BECKER, K., BENNETT, D., CLARIS, O., CREECH, C., DE LENCASTRE, H., DEIGHTON, M.,
631 DENIS, O., FERGUSON, J., HUANG, Y.-C., KLINGENBERG, C., INGEBRETSEN, A., LAFERRIÈRE, C., DOS
632 SANTOS, K., SCHRENZEL, J., SPILIOPOULOU, I., STEFANI, S., TAEKSOO, K., TARKKA, E., FRIEDRICH, A.,
633 VANDENBROUCKE-GRAULS, C., USSHER, J., VANDENESCH, F., WESTBLADE, L., LINDSAY, J.,
634 VANDENESCH, F., LARSEN, A., ZANGER, P., KAHL, B., AYMERICH, C., THE INTERNATIONAL
635 CONSORTIUM FOR STAPHYLOCOCCUS CAPITIS NEONATAL, S. & THE, E. S. G. O. E. 2020. Niche

636 specialization and spread of Staphylococcus capitis involved in neonatal sepsis. *Nature Microbiology,*
637 5**,** 735-745.

638

Figure 1 Population structure of *S. capitis*. A maximum likelihood (ML) tree based on core gene alignment from Roary. Three groups are indicated; Non NRCS-A isolates are highlighted in green, proto NRCS-A in orange, and NRCS-A, in pink. Country of isolation is indicated by the colour of tip branches; Germany (grey circles), UK (black circles). Body site of isolation are shown by coloured boxes; orange – neonatal skin, brown - neontal gut, red – neonatal bloodstream, green – healthy adult skin, blue – adult prosthetic joint, pink – adult bloodsteam. Antimicrobial resistance (AMR) genes are represented by red boxes (blank boxes represent absence of the corresponding gene). The percentage identity of *nsr* and *tarJ* in each strain (compared to the reference sequences present in CR01 and CR05 respectively using BLASTp) are shown as pie charts. MIC data for chlorhexidine (CHX, purple bars) and octenidine (OCT, yellow bars) are shown with the dotted lines representing 4 µg/mL of OCT or CHX.

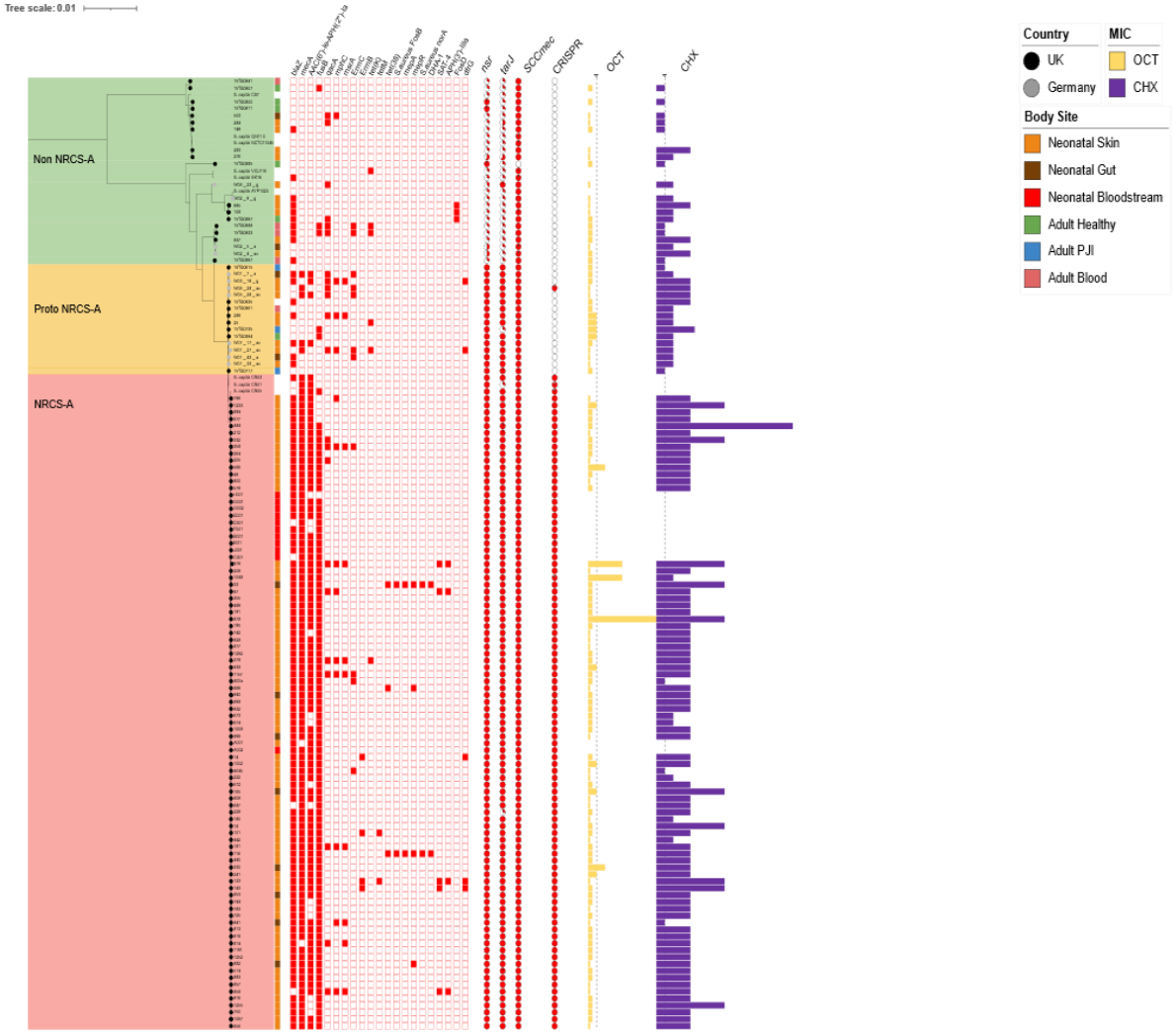

650 Figure 2. Detailed phylogeny of NRCS-A based on core SNP alignment. The week of isolation is indicated by
651 purple squares for all UK isolates and sources of each isolate are indicated by coloured squares (neonatal
652 skin = orange; neonatal gut = brown, neonatal bloodstream = red).

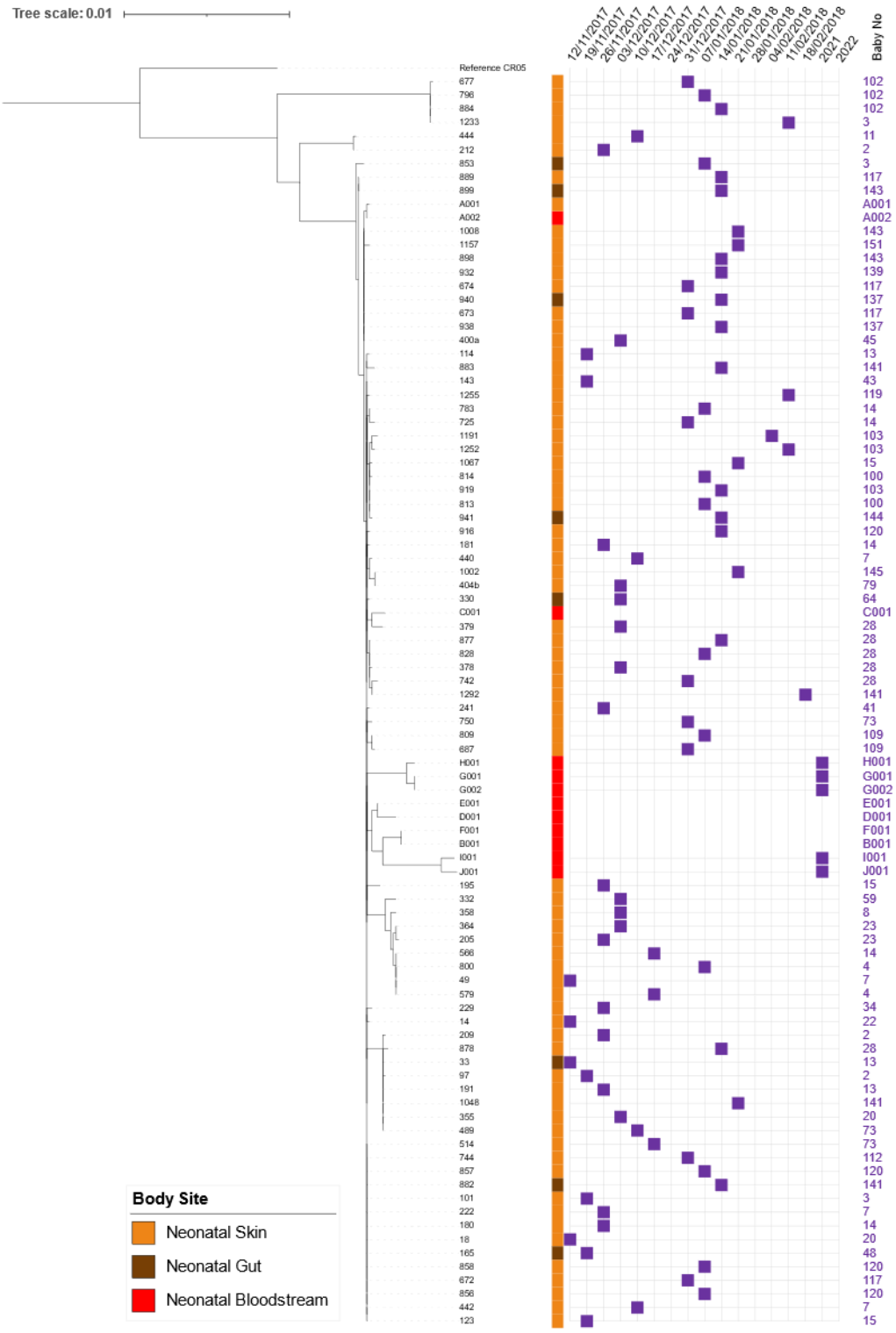

653

654 **Figure 3** Insertion of the CRISPR-Cas Type III-A system in NRCS-A isolates, compared to the related Proto
655 NRCS-A isolates.

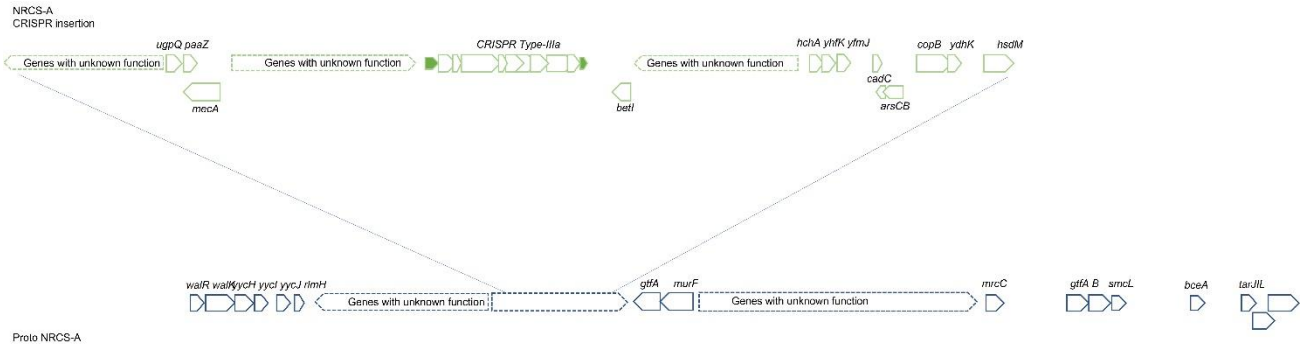

656

657 **Figure 4** Growth of *S. capitis* in different pH (pH7, 6 and 5.5), showing growth at final time point of 48 hours
658 from PM10 MicroPlate ™. Points indicate mean values and bars the standard error.

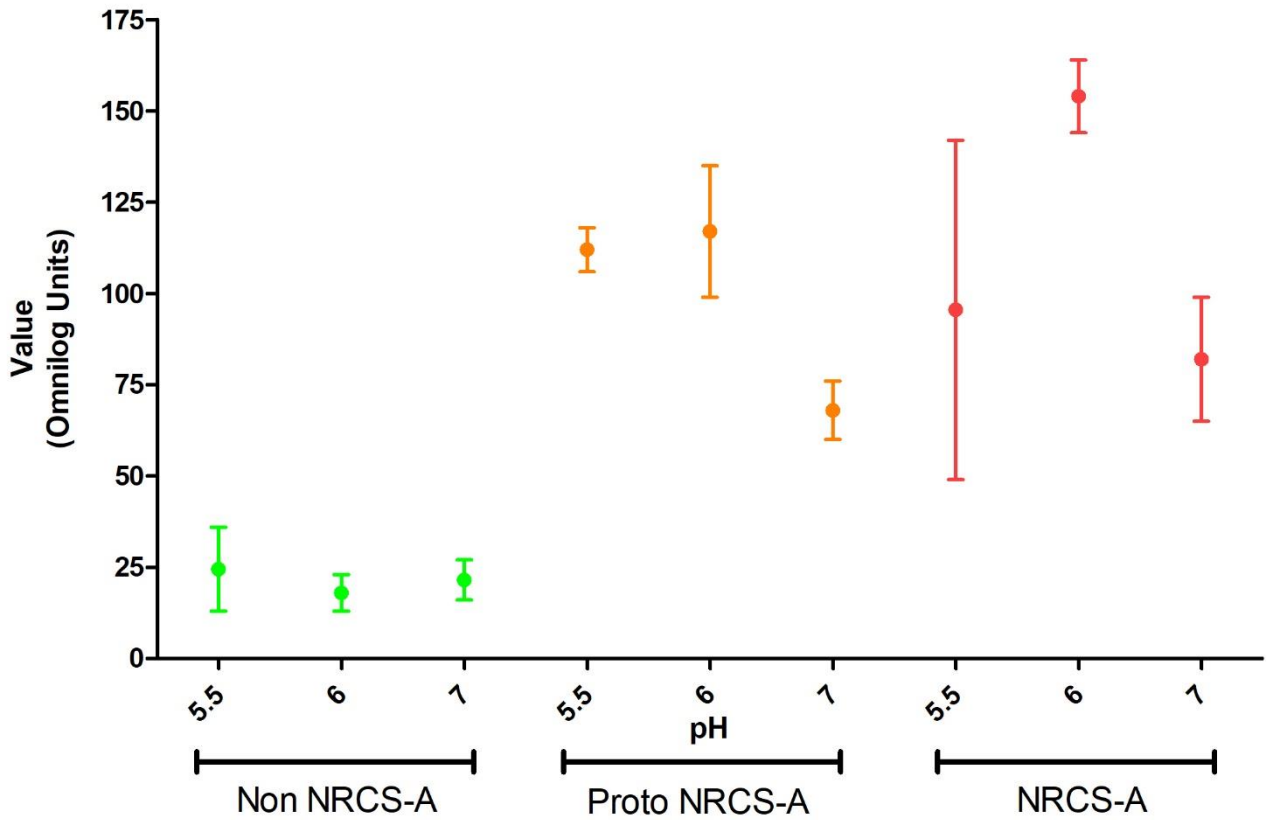

659

660

661 Figure 5 Chlorhexidine susceptibility of the three groups of *S. capitis*. Points represent values from individual
662 strains, horizontal lines indicate the means with bars showing the standard error of the mean.

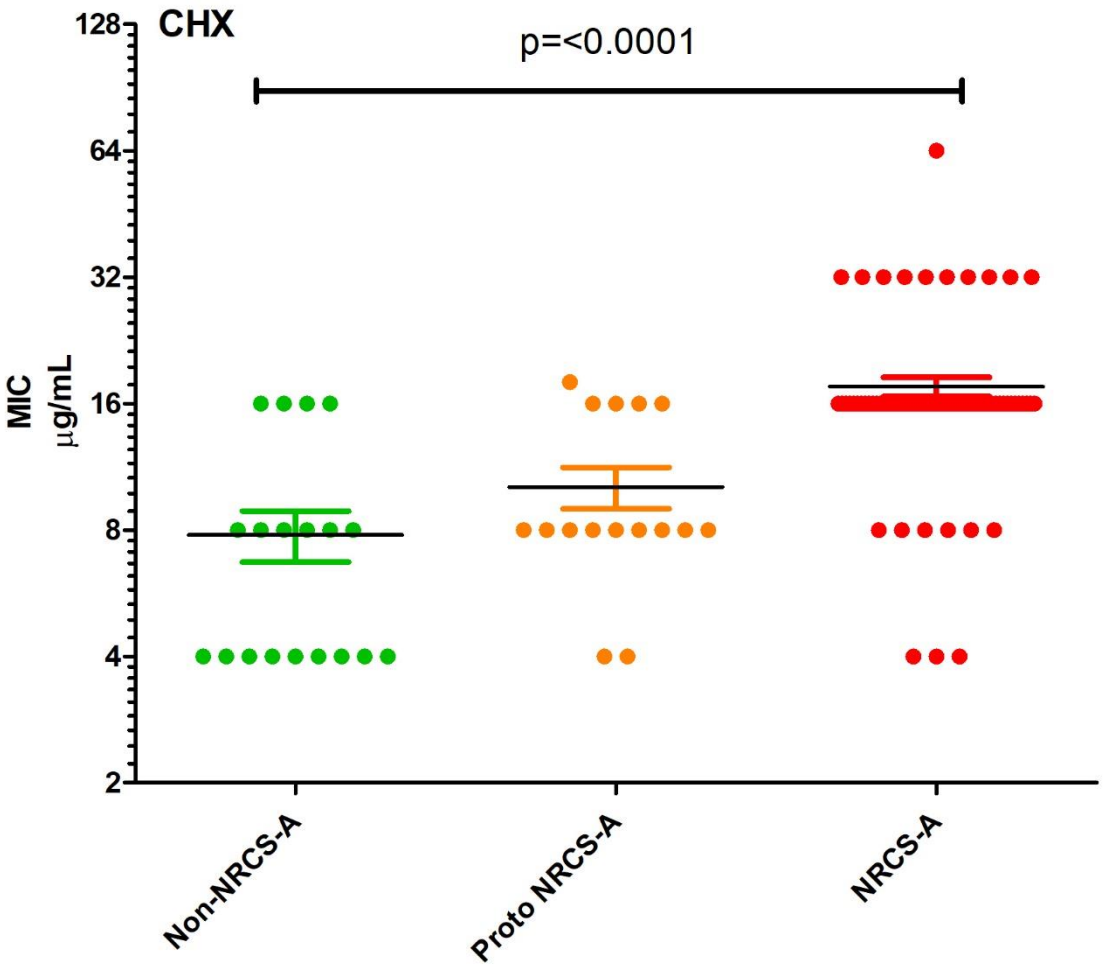

663

664 **Table 1** MIC^{50}- and MIC^{90} values of antimicrobials against the *S. capitis* groups.

	OCT		CHX		VAN		GEN		PEN		CEF		CIP		DAP		FUS	
	MIC^{50}	MIC^{90}	MIC^{50}	MIC^{90}	MIC^{50}	MIC^{90}	MIC^{50}	MIC^{90}	MIC^{50}	MIC^{90}	MIC^{50}	MIC^{90}	MIC^{50}	MIC^{90}	MIC^{50}	MIC^{90}	MIC^{50}	MIC^{90}
Non NRCS-A	2	2	8	16	1	2	0.064	32	0.5	8	1	4	0.5	4	0.5	2	2	2
Proto NRCS-A	2	4	8	16	1	2	1	32	2	32	1	4	0.25	0.5	0.5	1	0.064	2
NRCS-A	2	4	16	32	1	2	16	32	8	126	4	4	0.5	4	0.25	1	4	4
Overall	2	4	16	16	1	2	8	32	4	126	4	4	0.5	4	0.5	1	2	4
UK	2	4	16	32	1	2	8	32	4	126	4	4	0.5	4	0.5	1	4	4
German	1	2	8	16	1	1	8	32	4	126	4	4	0.5	4	0.5	1	2	2

665

666 **Table 2** Selected genes where presence/absence was strongly statistically associated with the NRCS-A
667 isolates compared other *S. capitis* clades.

Gene Presence	Annotation	Sensitivity	Specificity	Adjusted P value
cas 1, 2, 6, 10	CRISPR-associated endonucleases (subtype III-A)	100.00	100.00	9.42E-34
csm 2, 3, 4, 5, 6	CRISPR system Cms proteins	100.00	100.00	9.42E-34
ynfM	Inner membrane transport protein YnfM	97.94	100.00	2.97E-31
betI	HTH-type transcriptional regulator BetI	94.85	95.35	6.54E-25
paaZ	Bifunctional protein PaaZ	98.97	86.05	4.83E-24
ugpQ	Glycerophosphodiester phosphodiesterase cytoplasmic	98.97	86.05	4.83E-24
mecA	PBP2a family beta-lactam-resistant peptidoglycan transpeptidase MecA	98.97	83.72	6.37E-23
repB	Replication protein RepB	86.60	100.00	1.56E-22
trpS2	Tryptophan--tRNA ligase 2	82.47	100.00	2.97E-20
mntH	Divalent metal cation transporter MntH	91.75	90.70	7.06E-20
bcr	Bicyclomycin resistance protein	80.41	100.00	3.12E-19
copA	Copper-exporting P-type ATPase	96.91	74.42	1.10E-16
mcrC	Protein McrC	100.00	62.79	6.70E-16
copZ	Copper chaperone CopZ	95.88	74.42	7.84E-16
csoR	Copper-sensing transcriptional repressor CsoR	95.88	74.42	7.84E-16
czcD	Cadmium cobalt and zinc/H(+)-K(+) antiporter	95.88	74.42	7.84E-16
tarIJL	Ribitol-5-phosphate cytidylyltransferase,Ribulose-5-phosphate reductase, Teichoic acid ribitol-phosphate polymerase	100.00	60.47	4.08E-15
xerD	Tyrosine recombinase XerD	100.00	60.47	4.08E-15
nixA	Nickel transporter NixA	100.00	58.14	2.47E-14
lacE	PTS system lactose-specific EIICB component	97.94	62.79	1.66E-13
aacA-aphD	Bifunctional AAC/APH	76.29	90.70	4.90E-12
hchA	Protein/nucleic acid deglycase HchA	95.88	62.79	8.59E-12
yhfK	putative sugar epimerase YhfK	95.88	62.79	8.59E-12
appA	Oligopeptide-binding protein AppA	100.00	48.84	2.23E-11

yfmJ	Putative NADP-dependent oxidoreductase YfmJ	96.91	55.81	2.06E-10
dppB	Dipeptide transport system permease protein DppB	98.97	48.84	3.71E-10
hsdM	Type I restriction enzyme EcoKI M protein	87.63	69.77	2.40E-09
qorB	Quinone oxidoreductase 2	96.91	46.51	8.53E-08
gltC	HTH-type transcriptional regulator GltC	100.00	32.56	8.45E-07
gtfA	UDP-N-acetylglucosamine--peptide N-acetylglucosaminyltransferase GtfA subunit	100.00	32.56	8.45E-07
aes	Acetyl esterase	100.00	30.23	3.26E-06
cimH	Citrate/malate transporter	100.00	30.23	3.26E-06
cntABCDEF	Metal-staphylopine-binding proteins, permases and Staphylophine export/import proteins	100.00	30.23	3.26E-06
fabHB	3-oxoacyl-(acyl-carrier-protein) synthase 3 protein 2	100.00	30.23	3.26E-06
mleS	Malolactic enzyme	100.00	30.23	3.26E-06
mshD	Mycothiol acetyltransferase	100.00	27.91	8.12E-06
nmoA	Nitronate monooxygenase	100.00	27.91	8.12E-06
rl5	Polyphenol oxidase	100.00	27.91	8.12E-06
rutB	Peroxyureidoacrylate/ureidoacrylate amidohydrolase RutB	100.00	27.91	8.12E-06
cntKLM	Histidine racemase and Staphylopine synthase	100.00	25.58	3.10E-05
dppC	Dipeptide transport system permease protein DppC	87.63	53.49	3.22E-05
copB	Copper-exporting P-type ATPase B	91.75	41.86	0.0003
tarF	hypothetical protein	98.97	25.58	0.0003
gtfB	UDP-N-acetylglucosamine--peptide N-acetylglucosaminyltransferase stabilizing protein GtfB	92.78	39.53	0.0003
kdpD	Sensor protein KdpD	100.00	20.93	0.0004
cspA	Cold shock protein CspA	97.94	25.58	0.0012
efeM	putative iron uptake system component EfeM	100.00	16.28	0.0052
paiA	Spermidine/spermine N(1)-acetyltransferase	100.00	16.28	0.0052
hsdR	Type-1 restriction enzyme R protein	98.97	18.60	0.0094
dtd	D-aminoacyl-tRNA deacylase	100.00	13.95	0.0175
npr	NADH peroxidase	100.00	13.95	0.0175
clpB	Chaperone protein ClpB	93.81	27.91	0.0224

Gene Absence	**Annotation**	**Sensitivity**	**Specificity**	**Adjusted P value**

aaxC	Arginine/agmatine antiporter	0.00	62.79	4.85E-08
hdcA	Histidine decarboxylase proenzyme	0.00	62.79	4.85E-08
metNPQ	Methionine import ATP-binding protein, permease and putative D-methionine-binding lipoprotein	0.00	62.79	4.85E-08
gltR	HTH-type transcriptional regulator GltR	0.00	65.12	2.05E-07
dapL	LL-diaminopimelate aminotransferase	0.00	67.44	8.45E-07
pyrB	Aspartate carbamoyltransferase catalytic subunit	0.00	69.77	3.26E-06
argR	Arginine repressor	2.06	62.79	3.81E-06
pap	Polyphosphate:AMP phosphotransferase	2.06	62.79	3.81E-06
arsD	Arsenical resistance operon trans-acting repressor ArsD	0.00	72.09	8.12E-06
panS	Pantothenate precursors transporter PanS	0.00	72.09	8.12E-06
pfbA	Plasmin and fibronectin-binding protein A	0.00	72.09	8.12E-06
pncA	Nicotinamidase/pyrazinamidase	0.00	72.09	8.12E-06
wecD	dTDP-fucosamine acetyltransferase	0.00	72.09	8.12E-06
yclM	Aspartokinase 3	0.00	72.09	8.12E-06
arcA	Arginine deiminase	3.09	62.79	1.15E-05
arcR	HTH-type transcriptional regulator ArcR	0.00	74.42	3.10E-05
malP	PTS system maltose specific EIICB component	0.00	74.42	3.10E-05
tarM	Poly(ribitol-phosphate) alpha-N-acetylglucosaminyltransferase	0.00	74.42	3.10E-05
ydfJ	Membrane protein YdfJ	0.00	74.42	3.10E-05
arcC1	Carbamate kinase 1	4.12	62.79	4.28E-05
arsR	Arsenical resistance operon repressor	1.03	72.09	7.40E-05
nikE	Nickel import system ATP-binding protein NikE	0.00	76.74	0.0001
pnoA	Nitronate monooxygenase	0.00	76.74	0.0001
arcD	Arginine/ornithine antiporter	5.15	62.79	0.0001
relJ	Antitoxin RelJ	3.09	67.44	0.0001
arsA	Arsenical pump-driving ATPase	11.34	51.16	0.0001
kimA	Potassium transporter KimA	1.03	74.42	0.0003
argF	Ornithine carbamoyltransferase	6.19	62.79	0.0004
yoeB	Toxin YoeB	2.06	72.09	0.0004
dppE	Dipeptide-binding protein DppE	0.00	79.07	0.0004
bcrA	Bacitracin transport ATP-binding protein BcrA	4.12	67.44	0.0004
ktrB	Ktr system potassium uptake protein B	7.22	62.79	0.0009

merB	Alkylmercury lyase	0.00	81.40	0.0015
oppC	Oligopeptide transport system permease protein OppC	0.00	81.40	0.0015
sraP	Serine-rich adhesin for platelets	0.00	81.40	0.0015

668 Sensitivity and specificity of linkage with phenotypes calculated by Scoary based on Roary results. Adjusted P
669 value determined using Benjamini-Hochberg's method (Brynildsrud et al., 2016).

670

671

672 Table 3 Selected genes where presence was strongly statistically associated with the NRCS-A isolates
673 compared to the proto-NRCS-A isolates.

Gene	Annotation	Sensitivity	Specificity	P value
cas1, 2, 6, 10	CRISPR-associated endonucleases (type III-A)	100.00	100.00	1.81E-16
csm2,3,4,5,6	CRISPR system Cms proteins	100.00	100.00	1.81E-16
bceA	Bacitracin export ATP-binding protein BceA	100.00	93.75	6.26E-15
ynfM	Inner membrane transport protein YnfM	97.94	100.00	6.26E-15
smc	Chromosome partition protein Smc	96.91	100.00	3.07E-14
npr	NADH peroxidase	95.88	100.00	1.27E-13
lytO	putative autolysin LytO	95.88	100.00	1.27E-13
xerD	Tyrosine recombinase XerD	96.91	93.75	1.60E-12
araB	Ribulokinase	92.78	100.00	4.57E-12
cmoM	tRNA 5-carboxymethoxyuridine methyltransferase	90.72	100.00	3.45E-11
lexA	LexA repressor	90.72	100.00	3.45E-11
dut	Deoxyuridine 5'-triphosphate nucleotidohydrolase	88.66	100.00	1.87E-10
betI	HTH-type transcriptional regulator BetI	94.85	87.50	7.21E-10
repB	Replication protein RepB	86.60	100.00	9.40E-10
trpS2	Tryptophan--tRNA ligase 2	82.47	100.00	1.52E-08
mntH	Divalent metal cation transporter MntH	91.75	87.50	1.71E-08
hisC	Histidinol-phosphate aminotransferase	81.44	100.00	2.71E-08
bcr	Bicyclomycin resistance protein	80.41	100.00	4.93E-08
blaR1-2	beta-lactam sensor/signal transducer BlaR1	95.88	75.00	7.08E-08
hin	DNA-invertase hin	95.88	75.00	7.08E-08
ldh1	L-lactate dehydrogenase 1	78.35	100.00	1.41E-07
mecA	PBP2a family beta-lactam-resistant peptidoglycan transpeptidase MecA	98.97	62.50	1.59E-07
paaZ	Bifunctional protein PaaZ	98.97	62.50	1.59E-07
ugpQ	Glycerophosphodiester phosphodiesterase cytoplasmic	98.97	62.50	1.59E-07
blaI	Penicillinase repressor	93.81	75.00	6.17E-07
rhaS	HTH-type transcriptional activator RhaS	79.38	93.75	2.38E-06
blaZ	Beta-lactamase	84.54	87.50	2.55E-06

copA	Copper-exporting P-type ATPase	96.91	62.50	3.14E-06
copZ	Copper chaperone CopZ	95.88	62.50	9.94E-06
dtd	D-aminoacyl-tRNA deacylase	83.51	81.25	5.74E-05
menH	2-succinyl-6-hydroxy-2 4-cyclohexadiene-1-carboxylate synthase	93.81	62.50	6.91E-05
ydhP	Inner membrane transport protein YdhP	90.72	68.75	7.62E-05
csoR	Copper-sensing transcriptional repressor CsoR	95.88	56.25	9.74E-05
czcD	Cadmium cobalt and zinc/H(+)-K(+) antiporter	95.88	56.25	9.74E-05

674 Sensitivity and specificity of linkage with phenotypes calculated by scoary based on Roary results. Adjusted P
675 value (<0.001) determined using Benjamini-Hochberg's method (Brynildsrud et al., 2016).

676

677 **Table 4** Selected genes where presence was statistically associated with antibiotics and chlorhexidine
678 susceptibility.

		Adjusted P value		
Gene	**Annotation**	**CHX**	**PEN**	**CEF**
		16 µg/mL	**1 µg/mL**	**4 µg/mL**
aacA-aphD	Bifunctional AAC/APH	0.0001		
araB	Ribulokinase	2.47E-06		
bcr	Bicyclomycin resistance protein	7.49E-06		
betI	HTH-type transcriptional regulator BetI	1.57E-06		
bin3	Putative transposon Tn552 DNA-invertase bin3	2.79E-06	0.002	0.0126
blaI	Penicillinase repressor	3.50E-05		
blaR1-2	beta-lactam sensor/signal transducer BlaR1	0.000414331		
cas1,2,6,10	CRISPR-associated endonuclease Cas1	1.25E-07	0.002	0.0126
cls	Cardiolipin synthase	7.97E-05		
copA	Copper-exporting P-type ATPase	3.44E-06	0.002	0.0153
copZ	Copper chaperone CopZ	3.44E-06	0.002	0.0153
csm2,3,4,5,6	CRISPR system Cms protein Csm2	1.25E-07	0.002	0.0126
csoR	Copper-sensing transcriptional repressor CsoR	3.44E-06		
czcD	Cadmium cobalt and zinc/H(+)-K(+) antiporter	1.35E-06	0.003	
dut	Deoxyuridine 5'-triphosphate nucleotidohydrolase	7.83E-07	0.002	
hin	DNA-invertase hin	2.79E-06	0.002	0.0126
hisC	Histidinol-phosphate aminotransferase	7.49E-06		
ldh1	L-lactate dehydrogenase 1	3.06E-05		
lexA	LexA repressor	2.47E-06	0.002	
lytO	putative autolysin LytO	4.90E-05		
mboIR	hypothetical protein	1.25E-07		
mecA	PBP2a family beta-lactam-resistant peptidoglycan transpeptidase	1.20E-06		0.0126
mntH	Divalent metal cation transporter MntH	2.53E-06		0.0126
npr	NADH peroxidase	5.22E-06		
paaZ	Bifunctional protein PaaZ	3.34E-07		0.0126
repB	Replication protein RepB	0.0001		
rhaS	HTH-type transcriptional activator RhaS	1.02E-05		
rihC	Non-specific ribonucleoside hydrolase RihC		0.005	

smc	Chromosome partition protein Smc	1.25E-07	0.002	0.0126
trpS2	Tryptophan--tRNA ligase 2	2.79E-06		
ugpQ	Glycerophosphodiester phosphodiesterase cytoplasmic	3.34E-07		0.0126
xerC	Tyrosine recombinase XerC	1.25E-07	0.002	
xerD	Tyrosine recombinase XerD	1.24E-06		
ynfM	Inner membrane transport protein YnfM	1.25E-07	0.002	0.0126

679 A cut off MIC for chlorhexidine (CHX), penicillin (PEN) and cefotaxime (CEF) were used to distinguish
680 between strains with high and low tolerance (shown in Table 1). Adjusted P value determined using
681 Benjamini-Hochberg's method (Brynildsrud et al., 2016).

682 **Supplementary material**

683 **Supplementary Data 1** List of reference genomes of *S. capitis* strains used.

684 **Supplementary Data 2** Meta data for *Staphylococcus capitis* isolates. MICs OCT (octenidine range 1 – 32
685 µg/mL), CHX (chlorhexidine range 4 - 64 µg/mL), VAN (vancomycin range 0.25 - 4 µg/mL), GEN (gentamicin
686 range 0.016- 16 µg/mL), PEN (benzylpenicillin range 0.016 - 128 µg/mL), CEF (cefotaxime range 0.125 - 2
687 µg/mL), CIP (ciprofloxacin range 0.064 - 2µg/mL), DAP (daptomycin range 0.25 - 2 µg/mL), FUS (fusidic acid
688 range 0.064 -2 µg/mL). X indicates MIC data was not obtained.

689 **Supplementary Data 3** ABRICATE summary in Binary format, where 1 = ≥ 90% gene identity

690 **Supplementary Data 4** Snippy-core SNP distance matrix on all *S. capitis* collection using NRCS-A CR05 as the
691 reference genome.

692 **Supplementary Data 5** Snippy-core SNP distance matrix on NRCS-A isolates using CR05 as the reference
693 genome.

694 **Supplementary Data 6** Scoary report on NRCS-A traits compared to proto NRCS-A, Country (UK), cefoxitin ≥
695 4 µg/mL (CEF4), chlorhexidine ≥ 16 µg/mL (CHX 16), ciprofloxacin ≥ 2 µg/mL (CIP2), fusidic acid ≥ 2 µg/mL
696 (FUS2), gentamicin ≥ 8 µg/mL

697

698

699

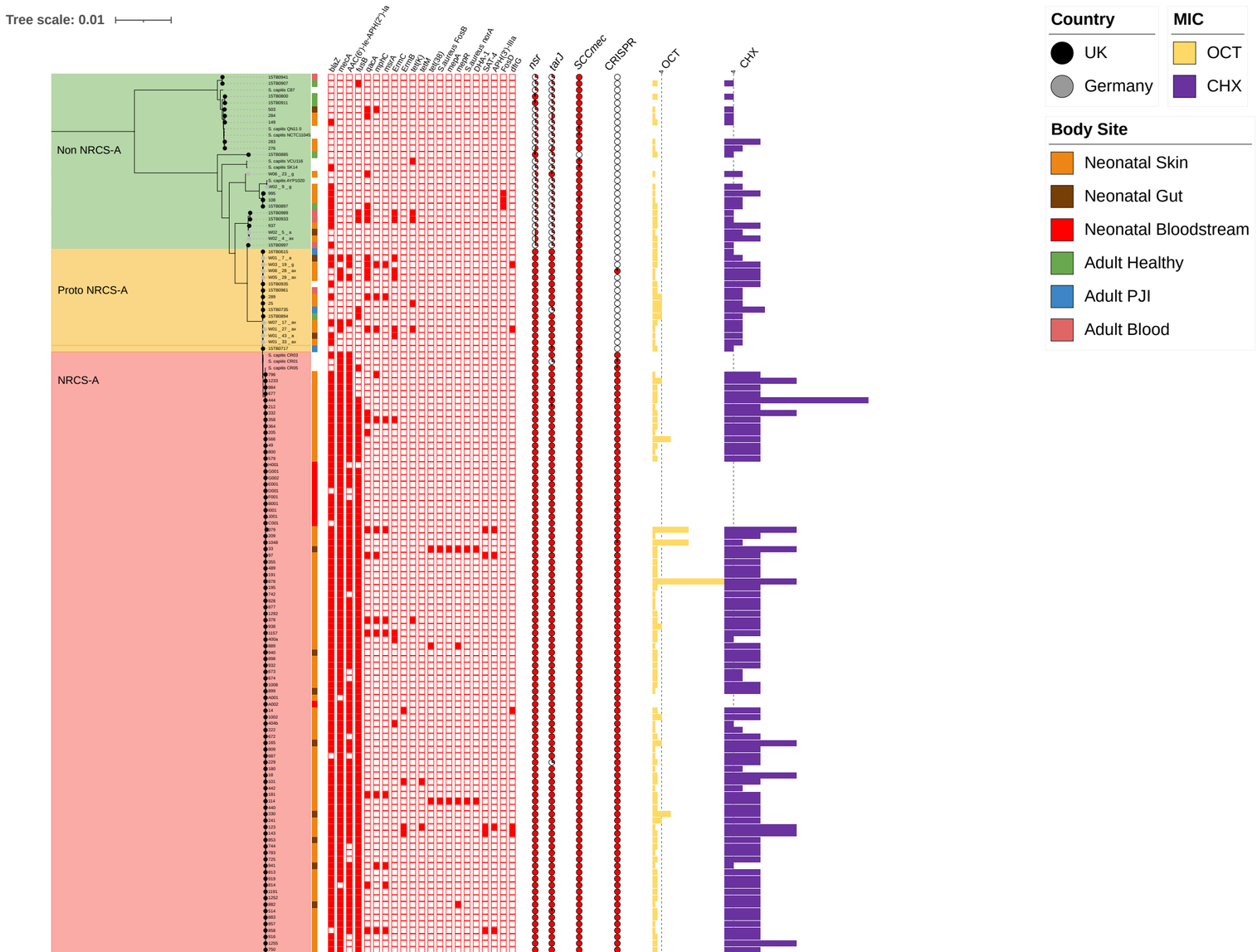

Country

- UK
- Germany

MIC

- OCT
- CHX

Body Site

- Neonatal Skin
- Neonatal Gut
- Neonatal Bloodstream
- Adult Healthy
- Adult PJI
- Adult Blood

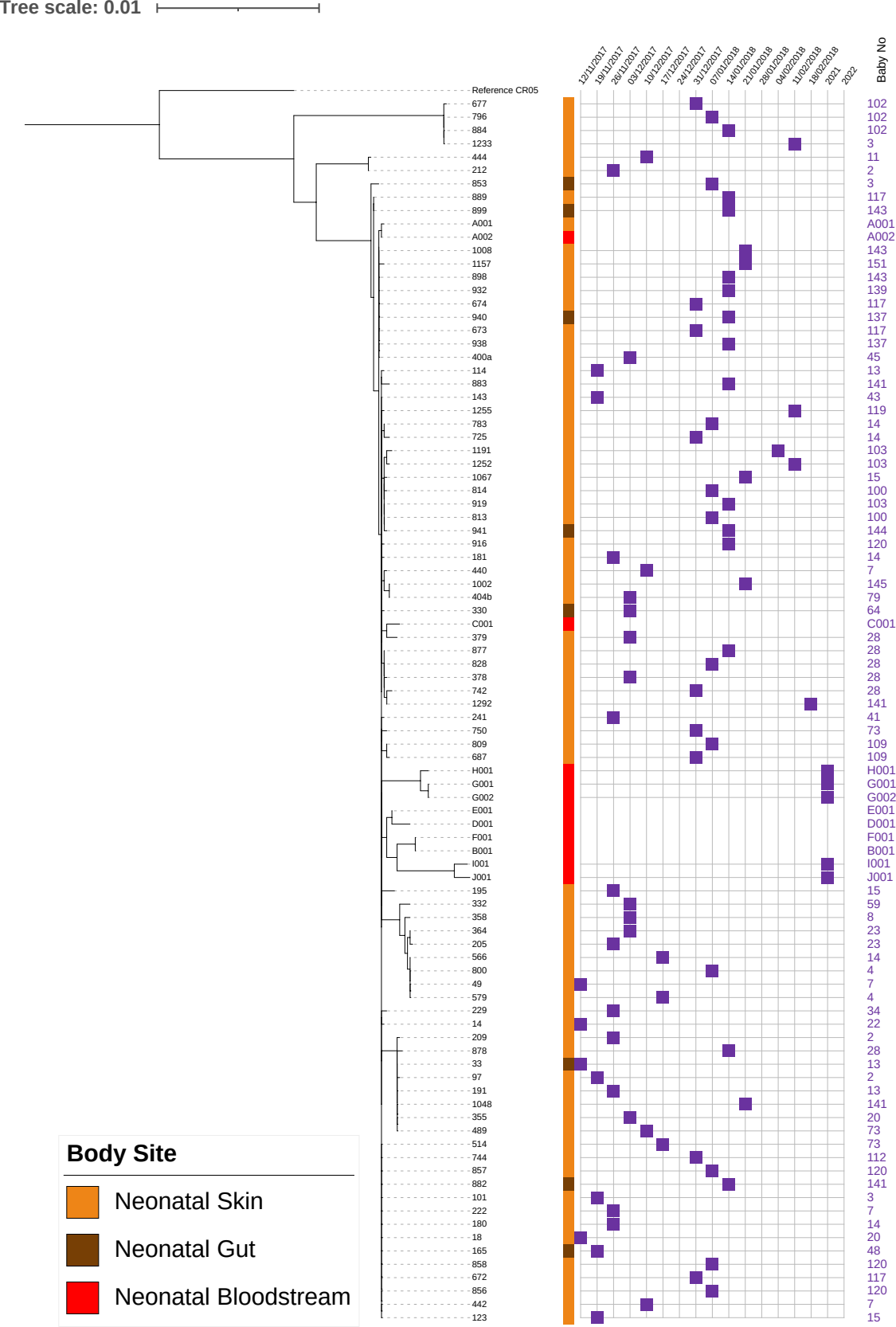
Tree scale: 0.01
12/11/2017
19/11/2017
26/11/2017
03/12/2017
10/12/2017
17/12/2017
24/12/2017
31/12/2017
07/01/2018
14/01/2018
21/01/2018
28/01/2018
04/02/2018
11/02/2018
18/02/2018
2021
2022
Baby No
Reference CR05
677 102
796 102
884 102
1233 3
444 11
212 2
853 3
889 117
899 143
A001 A001
A002 A002
1008 143
1157 151
898 143
932 139
674 117
940 137
673 117
938 137
400a 45
114 13
883 141
143 43
1255 119
783 14
725 14
1191 103
1252 103
1067 15
814 100
919 103
813 100
941 144
916 120
181 14
440 7
1002 145
404b 79
330 64
C001 C001
379 28
877 28
828 28
378 28
742 28
1292 141
241 41
750 73
809 109
687 109
H001 H001
G001 G001
G002 G002
E001 E001
D001 D001
F001 F001
B001 B001
I001 I001
J001 J001
195 15
332 59
358 8
364 23
205 23
566 14
800 4
49 7
579 4
229 34
14 22
209 2
878 28
33 13
97 2
191 13
1048 141
355 20
489 73
514 73
744 112
857 120
882 141
101 3
222 7
180 14
18 20
165 48
858 120
672 117
856 120
442 7
123 15
Body Site
Neonatal Skin
Neonatal Gut
Neonatal Bloodstream

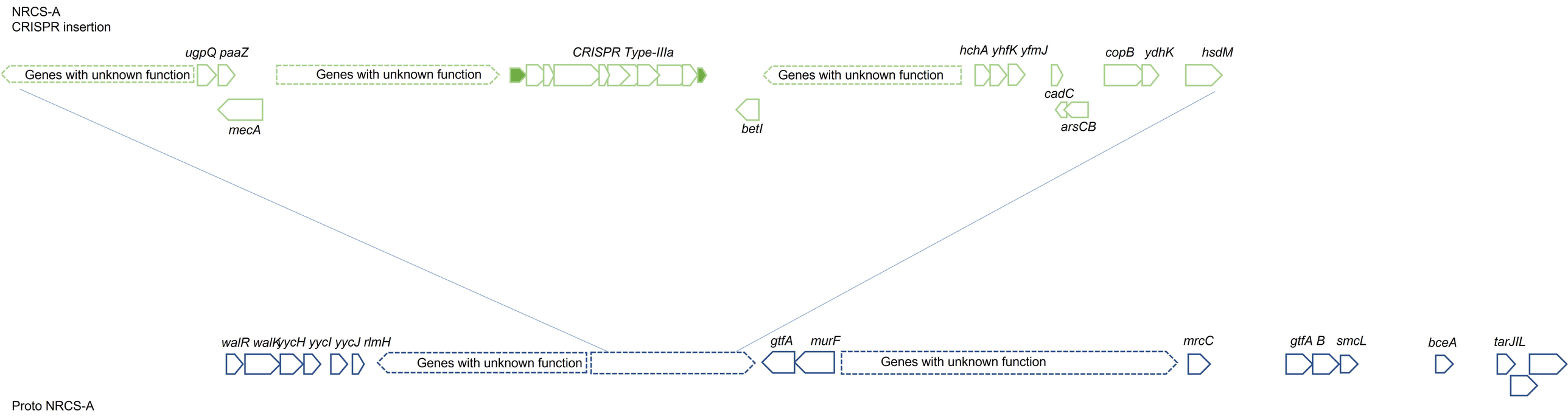
NRCS-A
CRISPR insertion
ugpQ paaZ
Genes with unknown function
Genes with unknown function
CRISPR Type-IIIa
Genes with unknown function
hchA yhfK yfmJ
copB ydhK
hsdM
cadC
mecA
betI
arsCB
walR walK yycH yycI yycJ rlmH
Genes with unknown function
gtfA murF
Genes with unknown function
mrcC
gtfA B smcL
bceA
tarJIL
Proto NRCS-A

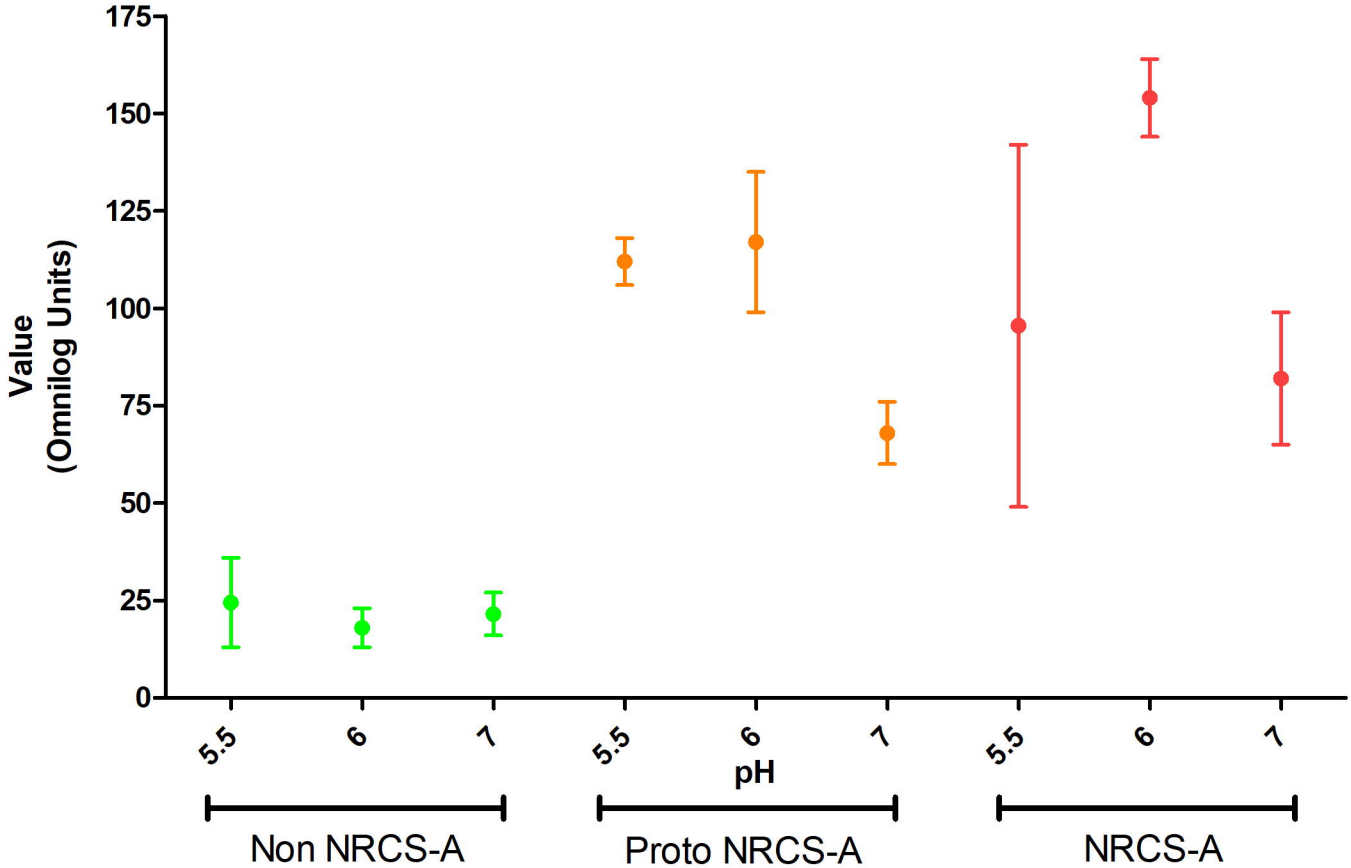
175
150
125
100
75
50
25
0
Value
(Omnilog Units)
5.5
6
7
5.5
6
7
5.5
6
7
pH
Non NRCS-A
Proto NRCS-A
NRCS-A

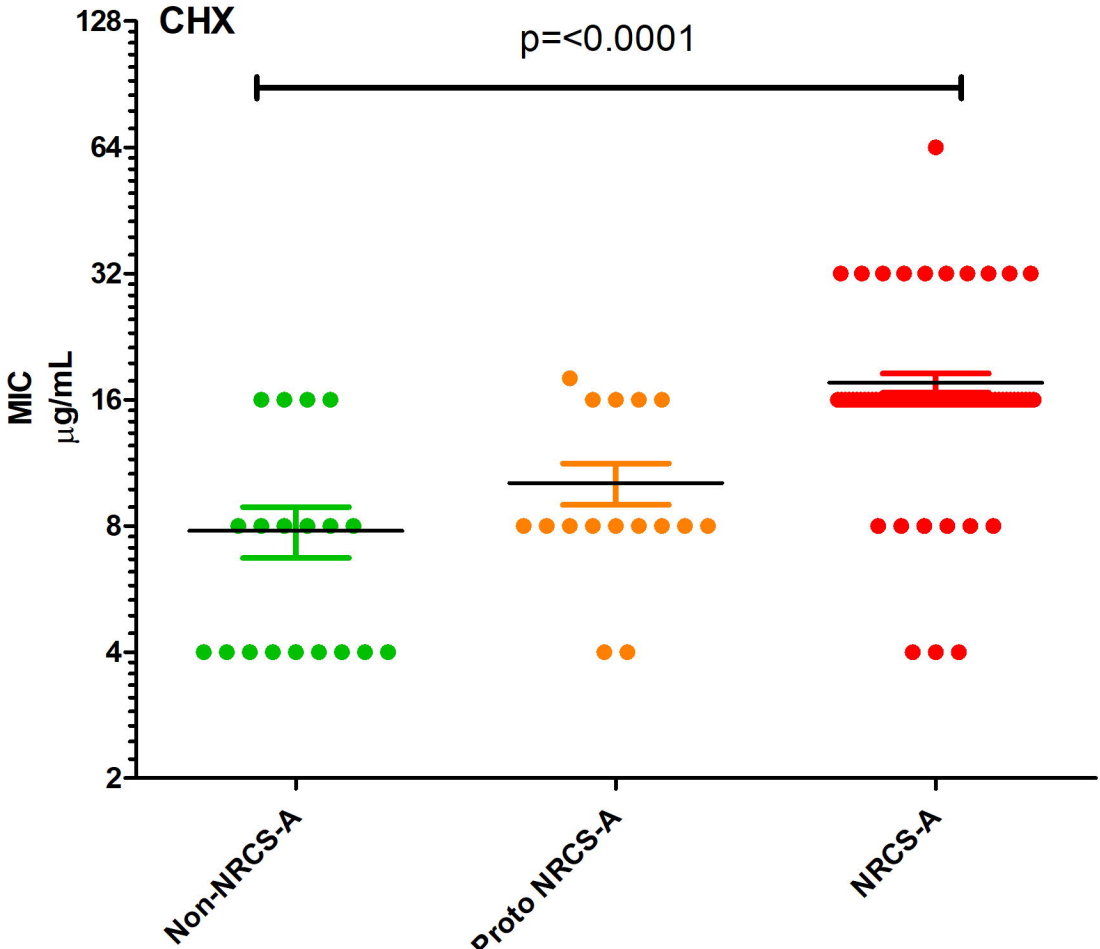
CHX
p=<0.0001
MIC
µg/mL
128
64
32
16
8
4
2
Non-NRCS-A
Proto NRCS-A
NRCS-A